Check for updates

Antibacterial activities against *Staphylococcus aureus* and *Escherichia coli* of extracted *Piper betle* leaf materials by disc diffusion assay and batch experiments

Pimploy Ngamsurach[ab] and Pornsawai Praipipat [ID] *[ab]

The use of contaminated water by bacteria may cause many diseases, and thus clean water is needed. Chlorine is normally used for the disinfection of wastewater treatment; however, it produces unwanted odors. Using extracted *Piper betle* (*P. betle*) is an interesting choice because it is a good chemical compound for bacterial inhibitions. This study attempted to extract *P. betle* leaf and synthesize *P. betle* beads (PBB) to characterize materials and investigate antibacterial efficiencies by disc diffusion assay, batch tests, adsorption isotherms, kinetics, and material reusability. The results demonstrated the successful extraction and synthesis of the materials of *P. betle*. *P. betle* powder (PBP) had porous and rough surfaces, whereas PBB had a spherical shape with a coarse surface. The four main chemical elements and functional groups of PBP and PBB were carbon, oxygen, calcium, chlorine, and O–H, C–H, N–H, C–O, respectively. The extraction yield and total phenolic, flavonoid, and tannin contents of *P. betle* were 11.30%, 201.55 $\pm$ 0.31 mg GAE per g, 56.86 $\pm$ 0.14 mg RE per g, and 41.76 $\pm$ 1.32 mg CE per g, respectively. The six main compounds of eugenol, quercetin, apigenin, kaempferol, ascorbic acid, and hydroxychavicol were detected by HPLC analysis. The results of the disc diffusion assay confirmed antibacterial efficiencies of PBB, and the batch tests examined high antibacterial efficiencies of PBB for 100% on *Staphylococcus aureus* and *Escherichia coli*. The adsorption isotherms and kinetics of PBB corresponded to Freundlich model and pseudo-second order kinetic model, and the desorption experiments confirmed the reusability of PBB. Therefore, PBB can be possibly applied for an antibacterial purpose in wastewater treatment systems.

Introduction

Water is one of main factors for living organisms; thus, access to clean water is necessary for a safe life. Because of increase in water consumption through many human activities such as household, industry, agriculture, and transportation, water pollution including bacterial contamination in water can occur.[1,2] Generally, bacteria are classified in two types, namely, Gram-positive and Gram-negative bacteria. *Staphylococcus aureus* (*S. aureus*) is normally represented as a Gram-positive bacteria, and it is also widely used for antibacterial experiments because of its high possibility of causing human diseases.[3] *Escherichia coli* (*E. coli*) is a common Gram-negative bacteria found in contaminated water as a pathogenic microorganism that causes human diseases, and it is also used as an indicator of water quality.[4] As a result, using water contaminated by bacteria may cause many diseases such as diarrhea, dysentery, typhoid fever, and septicemia. Therefore, water treatment is required before its safe use.

Ultraviolet light (UV), ozone, and chlorine are generally used for antibacterial treatment in a wastewater system with effective methods against many types of bacteria; however, these methods have the disadvantages of high operating costs, complicated maintenances, and unwanted odor after treatments.[5] Therefore, alternative methods have been studied to solve these problems. Many previous studies have investigated various alternatively antibacterial materials against *S. aureus* and *E. coli* in the form of nanomaterials with metal oxides of TiO_2, ZnO, CuO, MgO, iron oxide, silver nanoparticles (AgNPs), and green materials of various plant extractions with or without metal oxides as shown in Table 1. In Table 1, the antibacterial results of nanomaterials and green materials with metal oxides were closely related values. For green material comparison, their antibacterial activities of green materials with or without metal oxides had close values except that some studies of green materials with Ag or ZnO had higher values than others. However, the antibacterial materials of nanomaterials with metal oxides and green materials with metal oxides have the disadvantage of metal oxides harming the environment after treatment. As a result, an

Department of Environmental Science, Khon Kaen University, Khon Kaen, 40002, Thailand. E-mail: pornprai@kku.ac.th; pimploy@kkumail.com; Tel: +66 818774991

Environmental Applications of Recycled and Natural Materials (EARN) Laboratory, Khon Kaen University, Khon Kaen, 40002, Thailand

Table 1 Various alternative antibacterial materials against *S. aureus* and *E. coli* in nanomaterials with metal oxides and green materials

Methods/materials	*S. aureus/E. coli* Agar well diffusion (mm)	Disc diffusion (mm)	MIC (mg mL^{-1})	MBC (mg mL^{-1})	Applications	Ref.
Nanomaterials with metal oxides						
Chemical						
Ag NPs	—	12.1/13.5	0.075/0.05	—	Antibacterial activity	18
ZnO NPs	12.4 ± 0.1–17.0 ± 0.5 (*S. aureus*)	13.1 ± 0.7 to 17.7 ± 0.1	—	—	Antibacterial and anticancer activity	19
Mechanochemical						
CuO NPs	11.3–12.4/10.6–11.2	—	2.5/3.75	5/7.5	Antibacterial activity	20
Wet chemical reduction						
CuO NPs	—	—	0.25/1	—	Antibacterial activity	21
ZnO NPs	—	—	0.1 (*S. aureus*)	—	Antibacterial activity	22
Iron-oxide NPs	13–29/10–26	—	—	—	Antibacterial activity	22
Sol–gel						
Boron-doped TiO₂NPs	4.5–8.5 (*E. coli*)	—	—	—	Antibacterial activity	23
TiO₂–ZnO–MgO	12.00 ± 0.94 to 15.16 ± 0.30/14.00 ± 0.89 to 14.91 ± 0.66	—	—	—	Antibacterial activity	24
TiO₂NPs	0.8–2.55 (*S. aureus*)	—	—	—	Antibacterial activity and dye degradation (methylene blue)	25
Co-precipitation						
CuO-doped TiO₂NPs	3.25–4.85 (*S. aureus*)	—	—	—	Antibacterial activity	26
CuO–NiO–ZnO NPs	7.2/9	—	—	—	Antibacterial activity	26
Refluxing precursor						
ZnO NPs	1–14, 1–7 (*S. aureus*)	—	—	—	Antibacterial activity	27
Hydrothermal						
MgO NPs	7–11/8–12	—	0.0125–0.05/0.0125–0.06	—	Antibacterial activity and dye degradation (methyl orange)	28
Green materials						
Biosynthesis						
CuO NPs using actinomycetes	11.6 ± 0.57 to 19.6 ± 0.57 (*S. aureus*)	—	—	—	Antibacterial activity	29
Ag₂ONPs using *Lippia citriodora*	19 ± 0.02 (*S. aureus*)	—	—	—	Antibacterial activity and dye degradation (acid orange 8)	30
Green synthesis						
Ag NPs using *Carica papaya*	—	14 ± 0.31/15 ± 0.12	—	—	Antibacterial activity and dye degradation (blue CP and yellow 3RS)	31
Carica papaya extract	—	2 ± 0.42/5 ± 0.22	—	—		31
CuO NPs using *Ruellia tuberosa*	—	15.5/11	—	—	Antibacterial activity and dye degradation (crystal violet)	32
TiO₂NPs using *Artocarpus heterophyllus*	—	17/23	—	—	Antibacterial activity	33

Table 1 (Contd.)

Methods/materials	S. aureus/E. coli		MIC (mg mL^{-1})	MBC (mg mL^{-1})	Applications	Ref.
	Agar well diffusion (mm)	Disc diffusion (mm)				
ZnO NPs using *Ulva lactuca*	24.0 ± 1.0 (*E. coli*)	—	—	—	Antibacterial activity, photocatalytic dye (methylene blue) and mosquito larvicides	34
MgO NPs using *Phyllanthus emblica*	6.0 ± 0.29 to 14.0 ± 0.19/ 8.0 ± 0.24 to 15.0 ± 0.21	—	—	—	Antibacterial activity and degradation dye (evans blue)	35
Syzygium polyanthum L.	—	9.33 ± 0.52/7.00 ± 0.28	0.63/1.25	1.25/2.5	Antibacterial activity and food sanitizer	36
Syzygium antisepticum	—	—	0.125 (*S. aureus*)	0.5 (*S. aureus*)	Antibacterial activity (application in cooked chicken)	37
Lawsonia inermis	15.5 ± 0.5 to 21.3 ± 1.5/8.1 ± 0.4 to 12.1 ± 0.6	—	6.25 ± 0.0/1.5 ± 1.4	25.0 ± 0.0/12.00 ± 0.0	Antibacterial activity (application in wound infections)	38
Azadirachta indica	6.2 ± 0.3 to 8.2 ± 0.7/6.3 ± 0.3 to 7.4 ± 0.4	—	25.0 ± 0.0/83.3 ± 28.9	50.0 ± 0.0/ 100.00 ± 0.0		
Achyranthes aspera	6.3 ± 0.6 to 7.0 ± 1.0/6.8 ± 0.8 to 7.6 ± 0.5	—	50.0 ± 0.0/100.0 ± 0.0	100.0 ± 0.0/ 200.0 ± 0.0		

alternative of using green plant extractions without metal oxides may be better than nanomaterials and green materials with metal oxides for the antibacterial activities of Gram-positive and Gram-negative bacteria without a dangerous concern to the ecosystem because they are currently applied in many applications of food preservation, skincare products, hair, dental, cosmetics, and biopesticides.[6–11]

Many plants such as *Sechium edule*, *Piper sarmentosum*, *Mentha cordifolia*, *Limnophila aromatica*, *Polygonum odoratum*, *Garcinia cowa*, and *Piper betle* have chemical compounds such as rutin, catechin, and hydroxylchavicol; thus, they can possibly inhibit both Gram-positive bacteria (*Staphylococcus aureus*, *Staphylococcus epidermidis*, *Bacillus cereus*) and Gram-negative bacteria (*Escherichia coli*, *Klebsiella pneumonia*, *Pseudomonas aeruginosa*).[12,13] In particular, *Piper betle* (*P. betle*) is an interesting choice for an antibacterial agent for both bacteria types because its leaf has active chemical compounds such as phenols, alkaloids, carbohydrates, flavonoids, chavibetol, and eugenol.[14–17] Therefore, this study attempted to extract *P. betle* from powdered *P. betle* leaf, and then modify the extracted *P. betle* to a bead form as a novel antibacterial material from the applied engineering aspect. Moreover, their antibacterial efficiencies on *S. aureus* and *E. coli* were investigated through a series of batch experiments for possible disinfectant applications in wastewater treatment.

This study aimed to extract *P. betle* leaf for antibacterial activities against *S. aureus* and *E. coli* to synthesize and characterize *P. betle* powder (PBP) and beads (PBB), to identify the extraction yield and total phenolic, flavonoid, and tannin contents of extracted *P. betle* (EPB), to determine compounds of EPB, to examine disc diffusion assay of extracted EPB and PBB, and to investigate the antibacterial efficiencies of PBB by a series of batch experiments, adsorption isotherms, and kinetics. Finally, the material reusability was explored by desorption experiments.

Materials and methods

Raw material

Piper betle (*P. betle*) leaves in Piperaceae were used as raw materials that were collected from a plantation from Sakon Nakhon province, Thailand between March and April 2019, and then they were kept at room temperature.

Chemicals

All chemical reagents were of analytical grade without the purification, which were nutrient agar and nutrient broth (HiMedia, India), 99.9% ethanol (C_2H_5OH) (RCI Labscan, Thailand), 65% nitric acid (HNO_3) (Merck, Germany), sodium hydroxide (NaOH) (RCI Labscan, Thailand), 99.5% dimethyl sulfoxide (C_2H_6OS or DMSO) (SDFCL, India), sodium alginate (Merck, Germany), calcium chloride ($CaCl_2$) (KEMAUS, New Zealand), Folin-Ciocalteu reagent (Sigma-Aldrich, Germany), gallic acid (Sigma-Aldrich, Germany), rutin (Sigma-Aldrich, Germany), vanillin (Sigma-Aldrich, Germany), catechin (Sigma-Aldrich, Germany), sodium carbonate (Na_2CO_3) (Sigma-

Aldrich, Germany), aluminum chloride hexahydrate ($AlCl_3$) (Sigma-Aldrich, Germany), and hydrochloric acid (HCl) (Sigma-Aldrich, Germany). For HPLC analysis, the methanol (CH_3OH), ethanol, and standard chemicals of eugenol, quercetin, apigenin, kaempferol, ascorbic acid, hydroxychavicol, rutin, syringic acid, catechin, sinapic acid, *p*-coumaric acid, caffeic acid, ferrulic acid, myrecetin, and gallic acid were HPLC grade (Sigma-Aldrich, Germany). 1% sodium hydroxide (NaOH) (RCI Labscan, Thailand) and 1% nitric acid (HNO_3) (Merck, Germany) were used for pH adjustments.

Microorganisms

Two bacterial strains, namely, *Staphylococcus aureus* (DMST 562) and *Escherichia coli* (DMST 4212), which were procured from Department of Medical Sciences, Ministry of Public Health, Bangkok, Thailand (DMST), were used in this study.

Preparation of bacterial water sample

The water samples were prepared by diluting *S. aureus* or *E. coli* of 10^8 CFU mL^{-1} in sterile deionized water to obtain initial *S. aureus* or *E. coli* concentrations in the range from 10^4 to 10^7 CFU mL^{-1}.

Synthesis of materials

Fig. 1 demonstrated the synthesized steps of three materials, which were *P. betle* powder (PBP), the extracted *P. betle* (EPB),

and *P. betle* beads (PBB). The three steps included raw material preparation, plant extraction, and bead formation, and their details are clearly explained below.

Step 1: The raw material preparation. *P. betle* leaves were washed with tap water for removing contaminants, cut into small pieces, and dried in a hot air oven (Binder, FED 53, Germany) at 50 °C for 12 h. Then, the dried samples were ground to powder using the blender and sieved in 125 μm. These samples were called *P. betle* powder (PBP) and kept in a desiccator until use in step 2.[39]

Step 2: The plant extraction (0.1 g mL^{-1}). 10 g PBP was added to a 250 mL Erlenmeyer flask containing 100 mL ethanol, and it was mixed by an orbital shaker (GFL, 3020, Germany) for 24 h with a constant stirring speed of 200 rpm at room temperature. Then, the samples were filtered by a vacuum pump, evaporated by a rotary evaporator (BUCHI, RE-111 Rotavapor, Switzerland) of 50 °C, freeze-dried (LaboGene, Scanvac, Denmark), and kept at 4 °C until use. These extracted plants were called extracted *P. betle* (EPB).

Step 3: Bead formation. 2% w/v sodium alginate solution was prepared by a hot plate (Ingenieurbüro CAT, M. Zipperer GmbH, M 6, Germany) at 60 °C with a constant stirring speed of 200 rpm for 30 min. Next, EPB was added into sodium alginate solution, and the samples were homogenously mixed by a hot plate at 60 °C with a constant stirring of 250 rpm for 30 min. Then, 0.1 M $CaCl_2$ solutions were prepared for setting the beads. After that, the samples were added into 50 mL glass
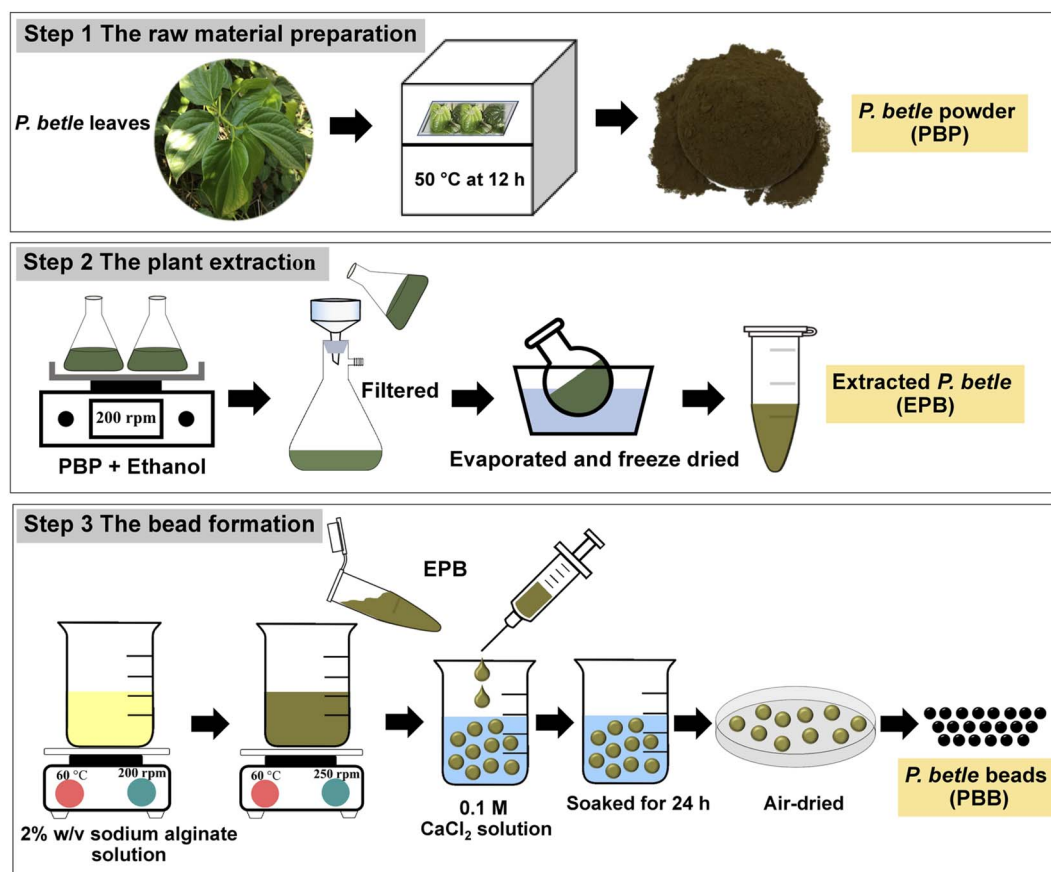

Fig. 1 The synthesized steps of three materials (PBP, EPB, and PBB).

syringe of 3 mm diameter and were added dropwise into 0.1 M $CaCl_2$ solution and soaked sample beads for 24 h. Finally, the sample beads were filtrated, rinsed with deionized water (DI), air-dried for 24 h, and kept in a desiccator before use. The sample beads were called *P. betle* beads (PBB).[39].

Note: The amount of EPB that was added into 2% w/v sodium alginate depended upon the concentration of the plant extract to the volume of the solvent solution prepared. For example, 0.1 g EPB was added into 1 mL 2% w/v sodium alginate for a concentration of 100 mg mL^{-1}.

Characterization of materials

Field Emission Scanning Electron Microscopy and Focus Ion Beam (FESEM-FIB) with Energy Dispersive X-Ray Spectrometer (EDX) (FEI, Helios NanoLab G3 CX, USA) were used to investigate the surface morphologies and chemical elements of materials, on which the samples were mounted on aluminum stubs by double-side carbon tapes and coated using a gold-coater for 4 min using a 108 auto Sputter Coater with thickness controller MTM-20 model (Cressington, Ted Pella Inc, USA) by analyzing at 10 kV accelerating voltage. The chemical functional groups of the materials were identified by Fourier Transform Infrared Spectroscopy (FTIR) (Bruker, TENSOR27, Hong Kong) in the range of 4000–600 cm^{-1} with a resolution of 4 cm^{-1} and 16 scans over the entire covered range.[39]

Determination of the extraction yield and total phenolic, flavonoid, and tannin contents of *P. betle*

The extraction yield in percentage was calculated using eqn (1).

$$\text{Yield (\%)} = W_c/W_r \times 100 \qquad (1)$$

where, W_c is weight of extracted *P. betle* (g) and W_r is weight of *P. betle* (g).

For the total phenolic content, a Folin-Ciocalteu assay was used in this study by modifying from the study of Singleton, V. L. *et al.*[40] 0.5 mg of the extracted P. betle, 2.5 mL of 10% Folin-Cioaclteu, and 2 mL of 7.5% Na_2CO_3 were added to a test tube. Then, it was vortexed and left at room temperature to react for 30 min. After that, the total phenolic content was measured by a UV-Vis spectrophotometer (Hitachi, UH5300, Japan) with a wavelength of 760 nm. Triplicate experiments were conducted for confirming the result. The average value was reported in mg gallic acid equivalent per gram of extracted *P. betle* (mg GAE per g).

For the total flavonoid content, a colorimetric assay was used in this study by modifying from Zhishen, J. *et al.*[41] 0.5 mg of the extracted *P. betle* and 2 mL of 2% $AlCl_3$ were added to a test tube. Then, it was vortexed and left at room temperature to react for 30 min. After that, the total flavonoid content was measured by a UV-Vis spectrophotometer with a wavelength of 420 nm. Triplicate experiments were conducted for confirming the result. The average value was reported in mg rutin equivalent per gram of extracted *P. betle* (mg RE per g).

For the total tannin content, a vanillin assay was used in this study by modifying from the study of Sun, B. *et al.*[42] 0.5 mg of the extracted *P. betle* and 5 mL of the mixed solution containing 4% $AlCl_3$ and 8% HCl were added to a test tube. Then, it was vortexed and left at room temperature to react for 30 min by keeping in the dark. After that, the total tannin content was measured by a UV-Vis spectrophotometer with a wavelength of 500 nm. Triplicate experiments were conducted for confirming the result. The average value was reported in mg catechin equivalent per gram of extracted *P. betle* (mg CE per g).

Determination compounds in extracted *P. betle* by HPLC analysis

For high-performance liquid chromatography (HPLC) (Agilent Technology, series 1220, USA), the HPLC column used was Discovery C18, 250 × 4.6 mm, with 5 μm of particle size (Sigma-Aldrich, Germany). 70 : 30 methanol–water solution was applied for setting the mobile phase with a flow rate of 1 mL min^{-1} for 20 min, and the UV detector was set at 280 nm. The stock standards of each compound were prepared from a ratio of 1 mg of standard : 1 mL of methanol. For sample preparation, 1 mg of extracted *P. betle* was dissolved in 1 mL ethanol, and then the sample was filtered by a 0.22 μm filter for injecting into the HPLC system. For HPLC analysis, 20 μL of the sample was injected into the HPLC system, triplicate experiments were applied, and the average was reported. Each standard was used under the same conditions with sample analysis for each compound.

Disc diffusion assay

EPB and PBB were used for disc diffusion assay, and the test details are shown in the diagram in Fig. 2. Three steps were applied, whose details are explained below; however, PBB skipped step 2.

Step 1: Preparation of bacteria concentration. Both bacterial types (*S. aureus* and *E. coli*) were prepared at 108 CFU mL^{-1} concentration using a 0.5 McFarland standard.

Step 2: Preparation of test solution. EPB was added into 10% DMSO solution in ratios of 100–400 mg mL^{-1}.

Step 3: The antibacterial tests. EPB and PBB were used for these experiments, and the method details explained below.

Step 3.1: EPB. For each plate test, the bacteria were applied to nutrient agar using the three-dimensional swab technique. Then, four pieces of paper disc, which were soaked into the test solution in step 2, were put in a plate test.

Step 3.2: PBB. For each plate test, bacteria were applied to nutrient agar using the three-dimensional swab technique. Then, four pieces of PBB were put in a plate test.

Then, the plates from steps 3.1 and 3.2 were taken in an incubation oven of 37 °C for 24 h. The results were analyzed by the diameter measurement of the inhibition zones. Triplicate experiments of each bacteria were used to confirm the results, and the average of the diameter of the inhibition zones was reported.

Antibacterial batch experiments

Antibacterial batch experiments were designed to investigate the influencing factors of dose, contact time, pH, and initial
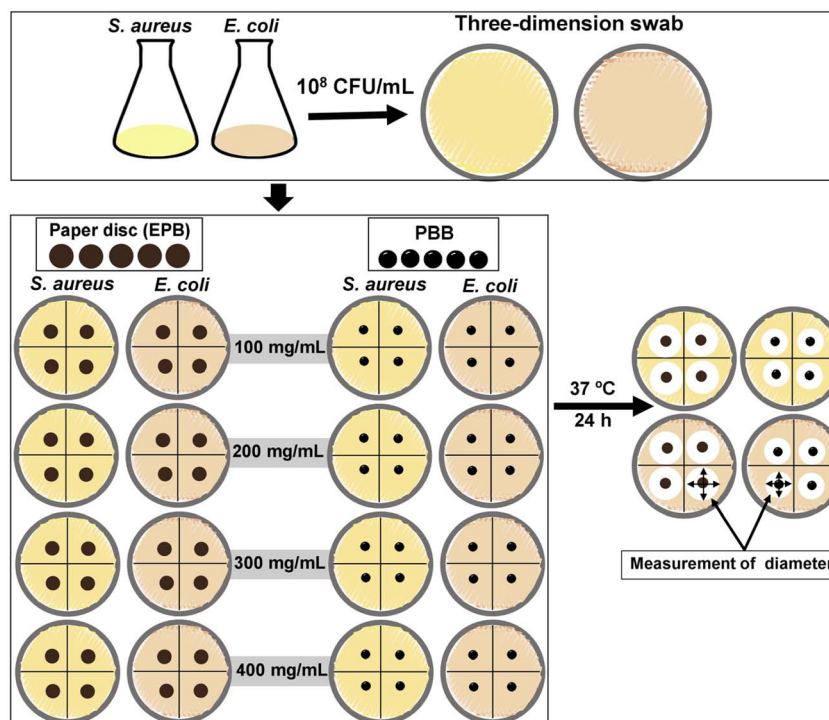
Fig. 2 Diagram of disc diffusion assay of EPB and PBB on *S. aureus* and *E. coli*.

bacteria concentration on the ability of PBB for inhibiting *S. aureus* and *E. coli* by a series of batch experiments. The influencing factors of material dosage of 0.1–0.4 g, contact time of 1–8 h, pH of 5, 7, and 9, and initial bacterial concentration of 10^4–10^7 CFU mL^{-1} were applied with the control condition of a bacterial concentration of 10^6 CFU mL^{-1}, a sample volume of 100 mL, a shaking speed of 200 rpm, and a temperature of 25 °C. The optimum condition of each influencing factor was used for a next sequencing batch experiment, in which the optimum condition was chosen from the lowest value of each influencing factor, which had the highest antibacterial efficiency of PBB. The results of the antibacterial batch experiments were confirmed by triplicate experiments of each influencing factor and their average values were reported. The plate count technique was used to analyze all the samples, and the percentage of antibacterial efficiency was calculated using eqn (2).

$$\text{Antibacterial efficiency (\%)} = ((C_0 - C_e)/C_0) \times 100 \quad (2)$$

where C_e is the equilibrium of the bacteria in the solution (CFU mL^{-1}) and C_0 is the initial bacteria concentration (CFU mL^{-1}).

Adsorption isotherms

Adsorption isotherms can be used to describe the interaction of the bacteria in the solution with PBB, which was analyzed using linear and non-linear Langmuir isotherm equations in (3) and (4) and Freundlich isotherm equations in (5) and (6), respectively.[43,44]

Langmuir isotherm:

Linear:

$$C_e/q_e = 1/q_m K_L + C_e/q_m \quad (3)$$

Non-linear:

$$q_e = q_m K_L C_e/1 + K_L C_e \quad (4)$$

Freundlich isotherm:
Linear:

$$\log q_e = \log K_F + 1/n \log C_e \quad (5)$$

Non-linear:

$$q_e = K_F C_e^{1/n} \quad (6)$$

where q_e is the capacity of bacterial adsorption on PBB at equilibrium (CFU g^{-1}), q_m is the maximum amount of bacteria adsorption on PBB (CFU g^{-1}), C_e is the equilibrium of bacterial concentration (CFU mL^{-1}), K_L is the adsorption constant (L CFU^{-1}), K_F is the constant of adsorption capacity (CFU g^{-1}) (L CFU^{-1})$^{1/n}$, and n is the constant depicting the adsorption intensity. Graphs of Langmuir and Freundlich isotherm models were plotted by linear plot features of C_e/q_e *versus* C_e and log q_e *versus* log C_e, respectively. For non-linear plot features of both the isotherm models, they were plotted by the capacity of bacterial adsorption on PBB at equilibrium (q_e) *versus* the equilibrium of bacterial concentration (C_e).

For the adsorption isotherm experiment, 0.3 g PBB was added to 250 mL Erlenmeyer flasks with variable bacterial concentrations

Fig. 3 Physical characteristics of *P. betle* in (a) leaf, (b) powder (PBP), and (c) beads (PBB).

in the range from 10^4 to 10^7 CFU mL^{-1}. The control condition was a sample volume of 100 mL, a contact time of 6 h, pH 7, a temperature of 25 °C, and a shaking speed of 200 rpm.

Adsorption kinetics

Adsorption kinetics can be used to explain the mechanism of antibacterial efficiency of PBB. The characteristic constants of sorption were investigated using linear and non-linear models of a pseudo-first order kinetic model following eqn (7) and (8) and a pseudo-second order kinetic model following eqn (9) and (10), respectively.[45,46]

Pseudo-first order kinetic model:

Linear:

$$\ln(q_e - q_t) = \ln q_e - k_1 t \qquad (7)$$

Non-linear:

$$q_t = q_e(1 - e^{-k_1 t}) \qquad (8)$$

Pseudo-second order kinetic model:

Linear:

$$t/q_t = 1/k_2 q_e^2 + (1/q_e)t \qquad (9)$$

Non-linear:

$$q_t = k_2 q_e^2 t/(1 + q_e k_2 t) \qquad (10)$$

where q_e (CFU g^{-1}) and q_t (CFU g^{-1}) are the volume of bacteria adsorbed by PBB at the equilibrium and at the time (t), respectively. k_1 (min^{-1}) and k_2 (g CFU^{-1} min^{-1}) are the reaction rate constant of pseudo-first order and pseudo-second order kinetic models, respectively. The graphs of pseudo-first order and pseudo-second order kinetic models were plotted by linear plot features of $\ln(q_e - q_t)$ and t/q_t *versus* time (t) for the difference of the initial bacterial concentrations. For non-linear plot features of both the kinetic models, they were plotted by the capacity of bacteria adsorbed PBB at the time (q_t) *versus* time (t).

For adsorption kinetics experiment, 3 g PBB were added to a 1000 mL beaker with a bacterial concentration of 10^6 CFU mL^{-1}. The control condition was a sample volume of 1000 mL, a contact time of 8 h, pH 7, a temperature of 25 °C, and a shaking speed of 200 rpm.

Desorption experiments

Desorption experiments were used to examine the possible reuse of PBB. After an adsorption process, PBB were desorbed using 100 mL 0.01 M HNO$_3$ solution with a shaking speed of 200 rpm for 2 h. After that, PBB was washed with deionized water and dried at room temperature. Then, PBB was ready for the next adsorption cycle. The desorption efficiency in percentage was calculated following eqn (11).

$$\text{Desorption (\%)} = (q_d/q_a) \times 100 \qquad (11)$$

where q_d is the amount of bacteria desorbed (CFU mL^{-1}) and q_a is the amount of bacteria adsorbed (CFU mL^{-1}).

Results and discussion

The physical characteristics of *P. betle*

P. betle is a member of the Piperaceae family, which is commonly grown in Southeast Asia such as Indian, Malaysia, Vietnam, Myanmar, Indonesia, and Thailand. It is a perennial with the height of 20 m and a diameter of 15–20 cm, whose fruit is fully concrescent and velutinous or woolly with 3–5 cm length. *P. betle* leaf is simple and alternate, and the leaf color is bright or dark green.[47] The physical characteristics of *P. betle* in leaf, powder, and bead forms used in this study are presented in Fig. 3a–c. The leaf is an ovate-shaped simple leaf and cordate leaf base with alternate leaf arrangement, as illustrated in Fig. 3a. Both sides of the leaf have smooth surfaces with a dark green color, but the upper surface has a glossier color than the lower surface. *P. betle* powder (PBP) has a dark green–brown color, whereas *P. betle* beads (PBB) has black colored beads, which are displayed in Fig. 3b and c, respectively.

Material characterization

FESEM-FIB and EDX analysis. The morphological structures of PBP and PBB were investigated by FESEM-FIB, as shown in Fig. 4a–c. PBP had porous and rough surfaces at 5000× magnification with 20 μm, whereas PBB had coarse surfaces at 5000× magnification with 10 μm, as shown in Fig. 4a and b. The shape of PBB has a spherical shape at 65× magnification with 1 mm, as shown in Fig. 4c. The chemical elements of PBP and PBB were examined by EDX analysis presented in Fig. 4d and e. The four main chemical compositions were found in both the materials, which were carbon (C), oxygen (O), calcium (Ca), and chloride
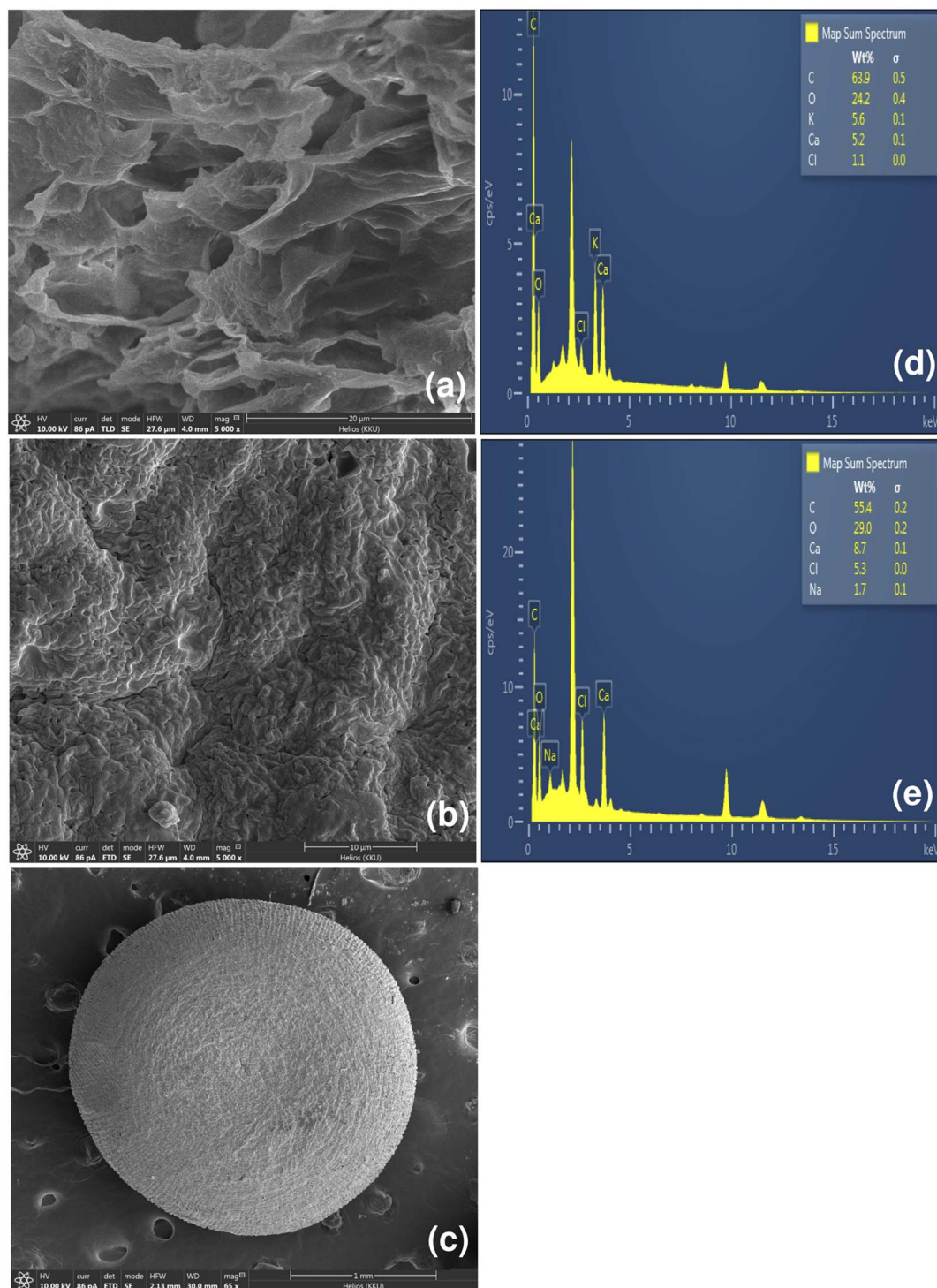
Fig. 4 FESEM-FIB images of surface morphologies of *P. betle* in (a) powder (PBP) at 5000× magnification, (b) beads (PBB) at 5000× magnification, (c) beads (PBB) at 65× magnification, and chemical compositions of *P. betle* in (e) powder (PBP) and (d) beads (PBB) by EDX analysis.

(Cl). Potassium (K) was only found in PBP, whereas sodium (Na) was only found in PBB because of the use of sodium alginate in bead formation. The mass in percentage by weight of each chemical components is demonstrated in Fig. 4d and e, and their four main chemicals were classified in order from high to low as C > O > Ca > Cl. In addition, K and Na were found at low concentrations, which had 5.6 wt% of K in PBP and 1.7 wt% of

Na in PBB, respectively. As a result, the changing form from the powder to the beads is affected by the changing of mass percentages in the chemical compositions of materials by increasing O, Ca, and Cl, whereas C was decreased. The increase in Ca and Cl might be from bead formation using $CaCl_2$.

FTIR analysis. The chemical functional groups of PBP and PBB were analyzed by FTIR in a broad peak range of 4000–
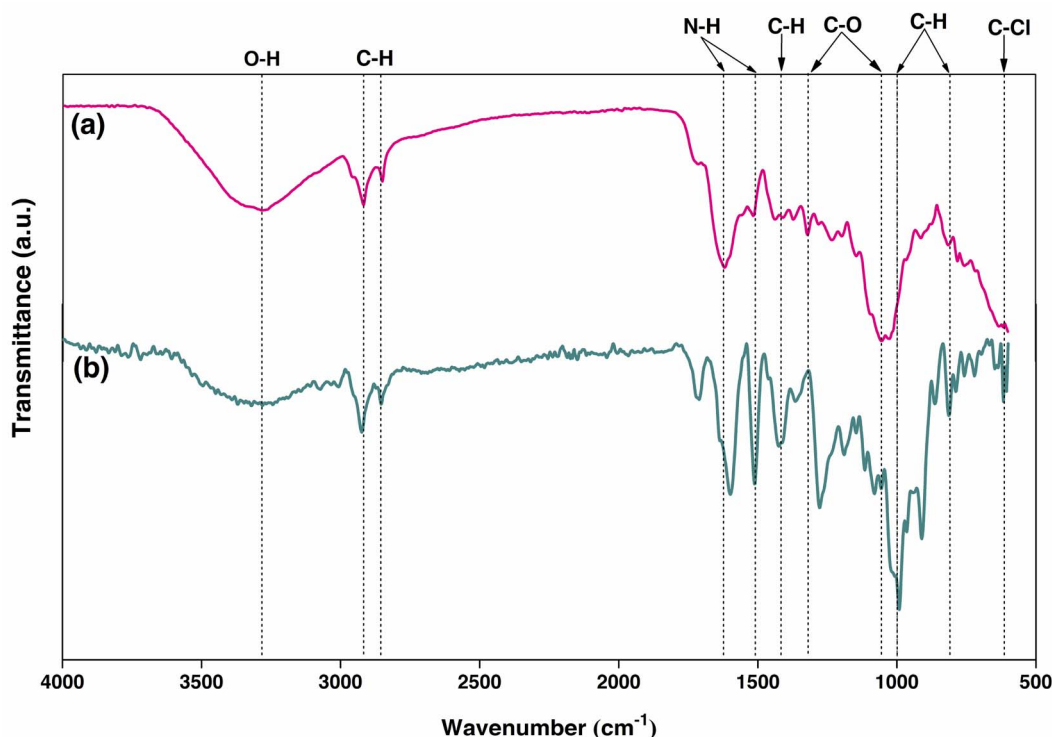
Fig. 5 FTIR spectra of (a) PBP and (b) PBB.

600 cm^{-1}, as represented in Fig. 5a and b. The four main chemical functional groups of both the materials were O–H, C–H, N–H, and C–O. O–H demonstrated the stretching arising from alcohols or phenolic compounds or carboxylic groups, which were generally found in many plant extracts and phenolic compounds, such as alkaloids, flavonoids in plant leaves, and also plays the important role of bacterial inhibition.[48,49] For C–H, it represented the stretching of alkanes or alkenes or bending of methyl groups (CH$_3$) or OOP bending of phenyl rings (aromatics), which could probably arise from the phenyl ring.[50,51] For N–H, it illustrated the bending of amide I or amide II, which are characteristics of proteins or enzymes in plants.[52,53] Finally, C–O indicated the stretching of alcohols, carboxylic acids, ethers, and esters.[54]

The chemical functional groups of PBP were observed for O–H at 3284.12 cm^{-1}, C–H at 2918.29 and 2850.69 cm^{-1}, N–H at 1618.94 cm^{-1}, and C–O at 1319.26 and 1054.06 cm^{-1}, which were similarly found in other studies with a little shift of the wavelengths.[50,52] For PBB, the chemical functional groups were presented for O–H at 3320.44 cm^{-1}, C–H at 2923.82, 1424.46, 991.75, 910.76, and 813.05 cm^{-1}, N–H at 1598.79 and 1511.29 cm^{-1}, and C–O at 1277.87 and 1189.70 cm^{-1}, and C–Cl at

617.30 cm^{-1}. As a result, the changing form from powder to beads is affected by changing the chemical functional groups of materials by only PBB found C–Cl (chloride compound) from the main chemical functional groups.

Determination of the extraction yield and total phenolic, flavonoid, and tannin contents of *P. betle*

The extraction yield and total phenolic, flavonoid, and tannin contents of *P. betle* demonstrated in Table 2. The extraction yield of *P. betle* was 11.30%. The total phenolic, flavonoid, and tannin contents of *P. betle* were 201.55 ± 0.31 mg GAE per g, 56.86 ± 0.14 mg RE per g, and 41.76 ± 1.32 mg CE per g, respectively, and these results were closely related to other previous studies for extracted *P. betle* by ethanol.[55–58]

Determination compounds in extracted *P. betle* by HPLC analysis

Several compounds were detected in extracted *P. betle* by HPLC analysis, as reported in Table 3. The six main compounds of eugenol, quercetin, apigenin, kaempferol, ascorbic acid, and hydroxychavicol were observed to be similarly found in previous

Table 2 The extraction yield and total phenolic, flavonoid, and tannin contents of *P. betle*

	Mean ± SD		
Extraction yield (%)	Total phenolic content (mg GAE per g)	Total flavonoid content (mg RE per g)	Total tannin content (mg CE per g)
11.30%	201.55 ± 0.31	56.86 ± 0.14	41.76 ± 1.32

Table 3   The compounds in extracted *P. betle* by HPLC analysis

Compound names	Content of compounds (mg g^{-1}) (mean ± SD)
Eugenol	18.06 ± 0.12
Quercetin	15.88 ± 0.15
Apigenin	5.15 ± 0.22
Kaempferol	2.77 ± 0.19
Ascorbic acid	1.86 ± 0.24
Hydroxychavicol	1.51 ± 0.17
Rutin	0.81 ± 0.08
Syringic acid	0.30 ± 0.04
Catechin	0.29 ± 0.05
Sinapic acid	0.26 ± 0.03
p-Coumaric acid	0.22 ± 0.07
Caffeic acid	0.14 ± 0.02
Ferrulic acid	0.06 ± 0.04
Myrecetin	0.04 ± 0.02
Gallic acid	0.03 ± 0.01

studies,[56] whereas the nine compounds, namely, rutin, syringic acid, catechin, sinapic acid, *p*-coumaric acid, caffeic acid, ferrulic acid, myrecetin, and gallic acid, were commonly found in small amounts correlated with the reports of other studies.[59]

Results of the disc diffusion assay

Disc diffusion assay is a method to examine the efficiency of extracted *P. betle* on specific organisms (*S. aureus* and *E. coli*). In this study, a paper disc was used as the preliminary test to determine the antibacterial efficiency on both bacterial types with varying concentrations of extracted *P. betle* in the range of 100–400 mg mL^{-1} before PBB was used to confirm the modified bead materials of extracted *P. betle* leaf. The results of disc diffusion assay are reported in Table 4 and Fig. 6.

For EPB, the average diameters of inhibition zones with varying EPB concentrations from 100 to 400 mg mL^{-1} on *S. aureus* and *E. coli* were 15.3 ± 1.0 and 22.5 ± 1.0, 21.2 ± 0.3 and 24.5 ± 1.3, 21.3 ± 1.3 and 24.6 ± 0.6, and 21.4 ± 1.2 and 24.7 ± 1.0 mm, respectively, and the average of four concentrations were 19.8 ± 3.0 and 24.1 ± 1.1 mm, respectively. As a result, their antibacterial efficiencies increased with increasing EPB concentrations, and they were constant at concentrations of 200–400 mg mL^{-1} with average values of 21.3 ± 0.1 and 24.6 ± 0.1 mm for *S. aureus* and *E. coli*, respectively. Moreover, EPB demonstrated higher antibacterial efficiency on *E. coli* than *S. aureus*. Since their average diameters of inhibition zones were the same value at 300 mg mL^{-1} EPB concentration, thus, 300 mg mL^{-1} was the optimum concentration for inhibition on both bacterial types.

Table 4   Disc diffusion assay by EPB and PBB on *S. aureus* and *E. coli*

Materials	The average diameter of inhibition zone (mm)			
	100 mg mL^{-1}	200 mg mL^{-1}	300 mg mL^{-1}	400 mg mL^{-1}
EPB *S. aureus*	15.3 ± 1.0	21.2 ± 0.3	21.3 ± 1.3	21.4 ± 1.2
E. coli	22.5 ± 1.0	24.5 ± 1.3	24.6 ± 0.6	24.7 ± 1.0
PBB *S. aureus*	11.4 ± 0.5	14.5 ± 0.7	15.7 ± 1.2	15.9 ± 0.4
E. coli	12.6 ± 0.6	15.4 ± 0.1	15.8 ± 0.9	16.0 ± 0.7

For PBB, the average diameters of the inhibition zones at varying EPB concentrations from 100 to 400 mg mL^{-1} on *S. aureus* and *E. coli* were 11.4 ± 0.5 and 12.6 ± 0.6, 14.5 ± 0.7 and 15.4 ± 0.1, 15.7 ± 1.2 and 15.8 ± 0.9, and 15.9 ± 0.4 and 16.0 ± 0.7 mm, respectively, and the average of four concentrations were 14.4 ± 2.1 and 15.0 ± 1.6 mm, respectively. As a result, their antibacterial efficiencies were increased with the increasing EPB concentrations, and they were constant at concentrations in the range of 200–400 mg mL^{-1} with average values of 15.4 ± 0.8 and 15.7 ± 0.5 mm for *S. aureus* and *E. coli*, respectively. In addition, PBB demonstrated higher antibacterial efficiency on *E. coli* than *S. aureus*, which agreed with the results from paper discs. Since their average diameters of the inhibition zones were nearly the same value at 300 mg mL^{-1} EPB concentration, thus 300 mg mL^{-1} was used as the optimum concentration for inhibitions on both bacterial types by PBB.

For comparing the results of the disc diffusion assay by EPB and PBB, the results of both materials demonstrated the same tendency of increasing antibacterial efficiency with increasing EPB concentration, and the EPB concentration of 300 mg mL^{-1} was the appropriate concentration for inhibition on *S. aureus* and *E. coli*. In deep consideration of the test material effect, two factors of diameter of the test materials and the interference of sodium alginate in bead materials might be a reason why the antibacterial activities of paper discs (EPB) were higher than PBB. For the diameter of the test materials, the diameter of paper disc (6 mm) was larger than the diameter of the glass syringe (3 mm) in bead formation; thus, it was possible that the paper disc might get a higher volume of extracted *P. betle* solution than bead materials, although the EPB concentrations were the same. For the interference of sodium alginate, the bead formation of extracted *P. betle* by sodium alginate might be an obstacle in the release of extracted *P. betle* for the antibacterial activity. However, the difference in the average diameters of inhibition zones with EPB concentrations of 100–400 mg mL^{-1} by paper disc (EPB) and PBB were not focused on because paper disc tests were only used as a preliminary confirmation of the ability of EPB against *S. aureus* and *E. coli*, whereas this study would focus on PBB for applying it in batch experiments.

Moreover, the comparison of the average diameter of the inhibition zone of the extracted *P. betle* leaf against *S. aureus* and *E. coli* to other previous studies with various extraction solutions is reported in Table 5. The six extracted solvents of methanol, ethyl acetate, petroleum ether, chloroform, water, and ethanol were used for *P. betle* extraction to inhibit *S. aureus* and *E. coli*. For *S. aureus*, the ethanol solvent demonstrated a higher antibacterial activity than the other solvents. EPB presented a higher zone of inhibition on *S. aureus* than other studies except the studies of Valle *et al.* and Khan J. A. and Kumar N.[16,60] On the other hand, PBB illustrated a higher or closer zone of inhibition on *S. aureus* than other studies except the studies of Valle *et al.* and Khan J. A. and Kumar N.[16,60] similar to EPB. As a result, ethanol was recommended as an extraction solvent to inhibit *S. aureus*. For *E. coli*, the methanol solvent demonstrated a higher antibacterial activity than other solvents; however, it presented a little higher zone of inhibition on *E. coli* than the ethanol solvent. EPB presented a higher zone
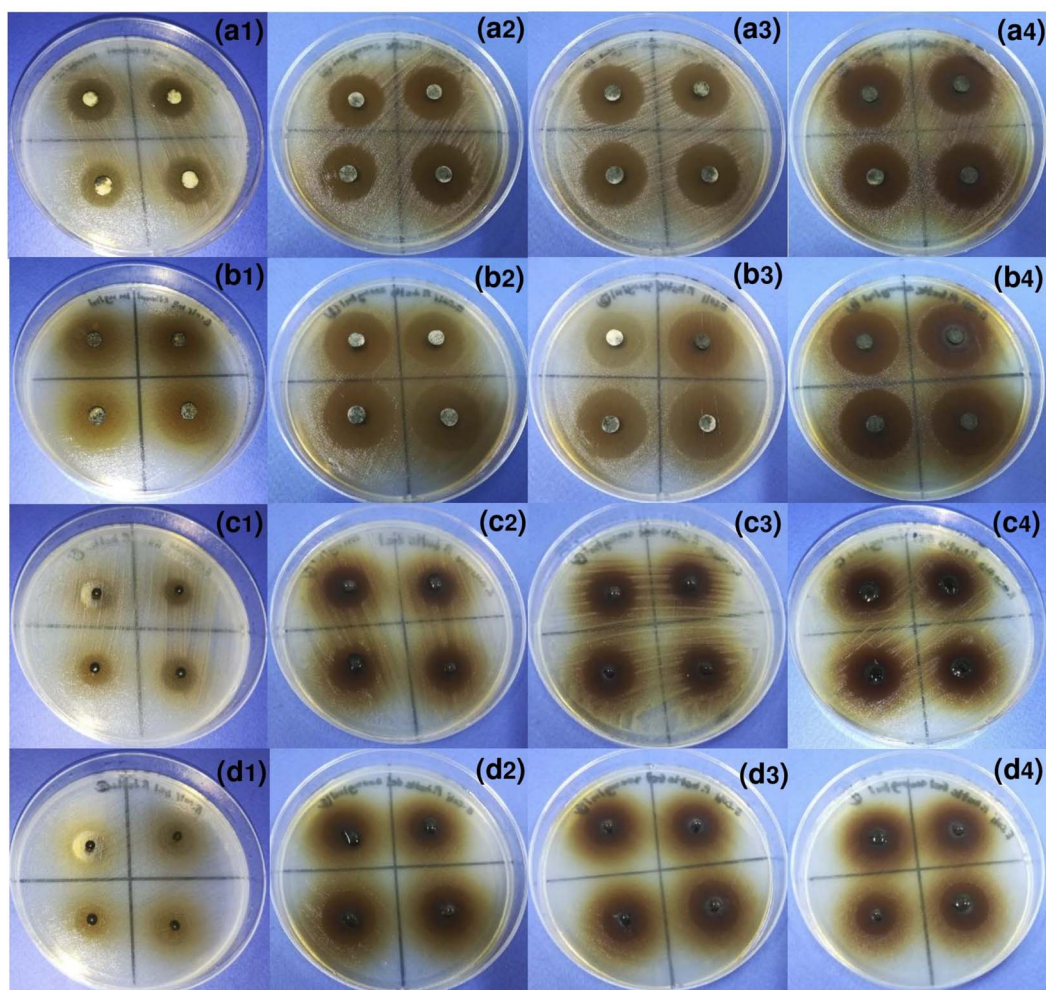
Fig. 6 The images of disc diffusion assay on *S. aureus* and *E. coli* by (a, b) EPB and (c, d) PBB in varying concentrations of (1) 100 mg mL^{-1}, (2) 200 mg mL^{-1}, (3) 300 mg mL^{-1}, and (4) 400 mg mL^{-1}.

of inhibition on *E. coli* than other studies except the study of Jayalakshmi B. *et al.*,[61] whereas PBB demonstrated a higher or closer zone of inhibition on *E. coli* than other studies except the studies of Jayalakshmi B. *et al.*, Valle D. L. *et al.*, and Kulnanan P. *et al.*[16,61,62]. Finally, since methanol is known as a more toxic solvent than ethanol, ethanol might be suitable for use as the extraction solvent of *P. betle* for the antibacterial activities on both *S. aureus* and *E. coli* more than methanol.

Therefore, the results of disc diffusion assay confirmed the abilities for inhibiting both bacterial types by EPB and PBB, and then, PBB was used to investigate the antibacterial efficiency by the batch tests with several affecting factors to confirm its efficiency to remove *S. aureus* and *E. coli* in water to study its possibly application for a disinfection process in the wastewater treatment system in the future.

The possible mechanisms of *S. aureus* and *E. coli* inhibition by extraction or beads materials (EPB and PBB)

Fig. 7 demonstrated the possible mechanisms of *S. aureus* and *E. coli* inhibition by EPB and PBB modified from a previous study.[39] For EPB, a paper disc soaked with extracted *P. betle* solution

contacted the cell bacteria in a plate test, and then the phenolic compounds, alkaloids, and flavonoids in the extracted *P. betle* that penetrated into the cell resulted in cell death by damaging the membrane, protein, DNA, and the main functions of bacteria.[71,72] For PBB, the same method was applied for the inhibition mechanism as that of EPB, but it only changed the material test from the paper disc to the extracted *P. betle* in the bead materials.

Therefore, using extracted *P. betle* by changing it a stable bead form may help to convenient apply it for the future wastewater treatment with easy separation after treatment instead of directly using extracted *P. betle*, which may be separated with difficulty from the treated wastewater, while the antibacterial batch experiments were designed to preliminarily prove this idea.

Antibacterial batch experiments

The effect of dosage. The effect of PBB dosages on bacterial removal efficiencies is represented in Fig. 8a. The antibacterial efficiencies of PBB on *S. aureus* and *E. coli* were increased with increasing dosages from 0.1 to 0.4 g. In Fig. 8a, 0.3 g and 0.4 PBB demonstrated high bacterial removal efficiencies of 100%, and

Table 5 Comparing the average diameter of inhibition zone of extracted *P. betle* leaf against *S. aureus* and *E. coli* to other previous studies with various extraction solvents

Solvents/methods	The average diameter of inhibition zone (mm)		
	S. aureus	*E. coli*	Reference
Methanol			
Agar well diffusion	25	15	60
	—	25.5 ± 0.28	61
Disc diffusion	—	23.5 ± 0.28	
	6.77 ± 0.25	8.53 ± 0.25	63
	—	19	64
	15.02 ± 0.27 to 21.03 ± 0.79	16.28 ± 0.19 to 16.40 ± 0.23	49
Ethyl acetate			
Agar well diffusion	—	20.25 ± 0.25	61
Disc diffusion	—	18.75 ± 0.47	
Petroleum ether			
Agar well diffusion	—	12.25 ± 1.03	
Disc diffusion	—	13.25 ± 0.28	
Chloroform			
Agar well diffusion	—	22.75 ± 0.47	
Disc diffusion	—	18.25 ± 0.25	
Water			
Agar well diffusion	—	18	65
	5.4 ± 0.01–12.3	8.5 ± 0.10	66
Ethanol			
Agar well diffusion	9.7 ± 0.02 to 18.0 ± 0.18	8.9 ± 0.21 to 11.0 ± 0.12	66
	16	17	60
	2.50 ± 5.00 to 20.38 ± 6.33	—	67
	9.5–15	11–17	57
	13.92–18.40	14.15–16.40	68
Disc diffusion	30	16	16
	10.5 ± 0.8		69
	15.06 ± 0.57 to 19.02 ± 0.74	14.93 ± 0.51 to 15.01 ± 0.57	49
	8 ± 0.25–13 ± 0.43		70
	—	20	64
	—	20.00–0.00	62
EPB	15.3 ± 1.0–21.4 ± 1.2	22.5 ± 1.0–24.7 ± 1.0	This study
PBB	11.4 ± 0.5–15.9 ± 0.4	12.6 ± 0.6–16.0 ± 0.7	This study

the PBB efficiencies were a little increased with increasing doses from 0.1 to 0.3 g. As a result, PBB was a high potential material to inhibit both bacterial types with almost 100% bacterial removal. Therefore, 0.3 g was the optimum dosage of PBB to inhibit *S. aureus* and *E. coli*, and was used to study the effect of contact time.

The effect of contact time. The contact time was varied from 1 to 8 h to examine the effect of contact time on the antibacterial efficiency of PBB on *S. aureus* and *E. coli*, as shown in Fig. 8b. The results illustrated that all the contact times presented high bacterial removal efficiencies of PBB more than 99% on both

the bacterial types, which were a little increased with increasing contact time. Moreover, the bacterial removal efficiencies of PBB from 5 to 8 h represented almost 100% bacteria removal with a nearly constant tendency, and 6 h was appropriately chosen as the middle value of this constant trend. Therefore, the optimum condition of PBB against both bacterial types was 0.3 g and 6 h, and was used for the effect of pH.

The effect of pH. While dosage and contact time are interesting factors for exploring the bacterial removal efficiency of PBB against *S. aureus* and *E. coli*, the pH should not be ignored as an important influencing factor. Fig. 8c examined the results of pH effect of pH 5, 7, and 9 on both bacterial types, in which PBB presented high efficiencies of almost 100% to inhibit *S. aureus* and *E. coli* in all pH conditions (acidic, neutral, and basic); thus, the pH did not affect the PBB efficiency. To deeply consider the pH effect on both bacterial types, the bacterial removal efficiencies of PBB on *S. aureus* were a little increased with increasing pH value, and at pH 9, the highest bacterial removal was obtained. As a result, the basic condition was preferred for *S. aureus* inhibition by PBB. For *E. coli*, the highest antibacterial efficiency of PBB of 100% was demonstrated at pH 7, and its efficiency decreased at pH 9; thus, pH 7 was the perfect condition and chosen as the optimum pH of both bacterial types because of safe water quality reason. Therefore, the optimum conditions of PBB were 0.3 g, 6 h, and pH 7, which were used to study the effect of concentration.

The effect of concentration. The results of the effect of concentration from 10^4 to 10^7 CFU mL^{-1} of both the bacterial types is demonstrated in Fig. 8d. PBB confirmed a high potential material for 100% bacterial removal on *S. aureus* and *E. coli* from 10^4 to 10^6 CFU mL^{-1}. The antibacterial efficiency on *S. aureus* was a little decreased at a concentration of 10^7 CFU mL^{-1}, while *E. coli* had a constant value of 100% bacterial removal. Therefore, 10^6 CFU mL^{-1} was confirmed as a suitable concentration to inhibit on both bacterial types.

In conclusion, the material dosage had a higher influence on the bacterial removal efficiencies of PBB on both bacterial types than the contact time, pH, and concentration, and the optimum condition of PBB to inhibit *S. aureus* and *E. coli* was 0.3 g, 6 h, pH 7, and 10^6 CFU mL^{-1} for 100% bacterial removal. On comparing with a previous study,[39] the optimum condition of this study had a similar material dose of 0.3 g and pH of 7 with the previous study for 100% inhibition of *S. aureus* and *E. coli*, whereas this study spent a contact time of 6 h more than the previous study, which was 3 h and 2 h for *S. aureus* and *E. coli*, respectively, possibly resulting from the use of different plants.

Adsorption isotherms

The adsorption isotherm studies of PBB on *S. aureus* and *E. coli* with the fitting of linear and non-linear Langmuir and Freundlich models are demonstrated in Fig. 9. For the linear model, the Langmuir model was plotted for C_e/q_e versus C_e, whereas the Freundlich model was plotted for log q_e versus log C_e. For the non-linear model, both the models were plotted as q_e versus C_e. In addition, the equilibrium isotherm parameters are reported in Table 6.
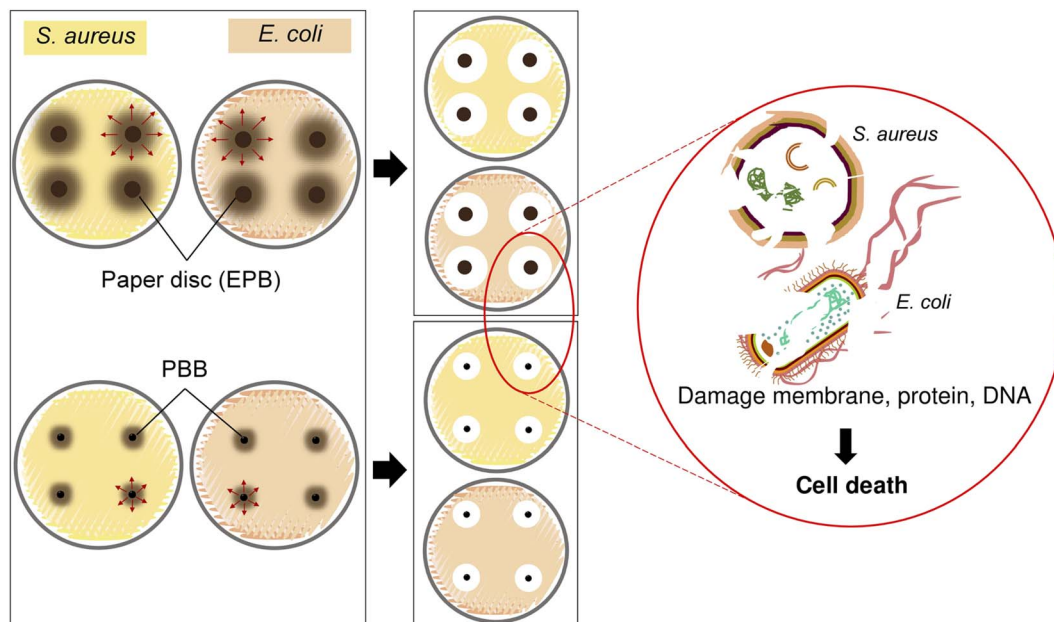
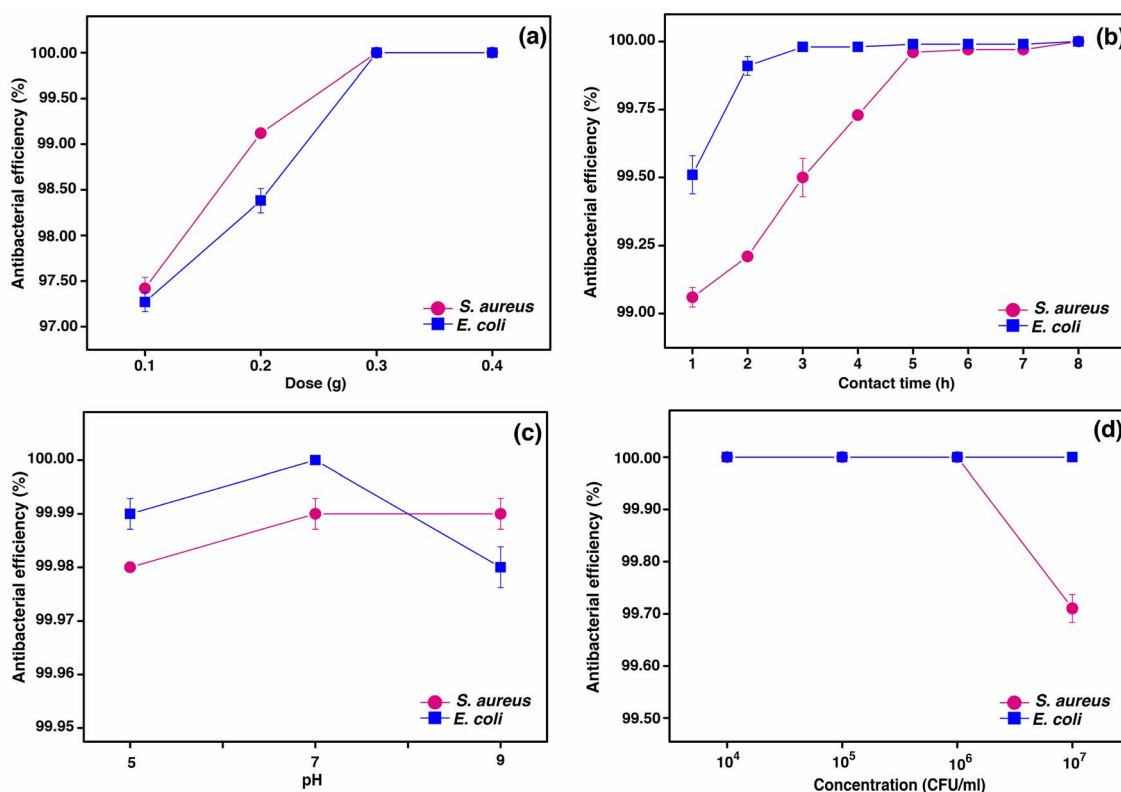Fig. 7 The possible mechanisms of *S. aureus* and *E. coli* inhibitions by EPB and PBB.

Fig. 8 Antibacterial batch experiments of PBB in (a) dose, (b) contact time, (c) pH, and (d) concentration on *S. aureus* and *E. coli*.

For the Langmuir linear model, the maximum adsorption capacity (q_m) of PBB on *S. aureus* and *E. coli* was 1×10^{10} and 1.4286×10^{10} CFU g^{-1}, respectively, and the Langmuir linear adsorption constants (K_L) of PBB were 0.0003 and 0.0004 L CFU^{-1} for *S. aureus* and *E. coli*, respectively. For the Langmuir

non-linear model, the maximum adsorption capacity (q_m) of PBB on *S. aureus* and *E. coli* was 1.0083×10^{10} and 1.4404×10^{10} CFU g^{-1}, respectively, and the Langmuir non-linear adsorption constants (K_L) of PBB were 0.0002 and 0.0003 L CFU^{-1} for *S. aureus* and *E. coli*, respectively. The R^2 of Langmuir
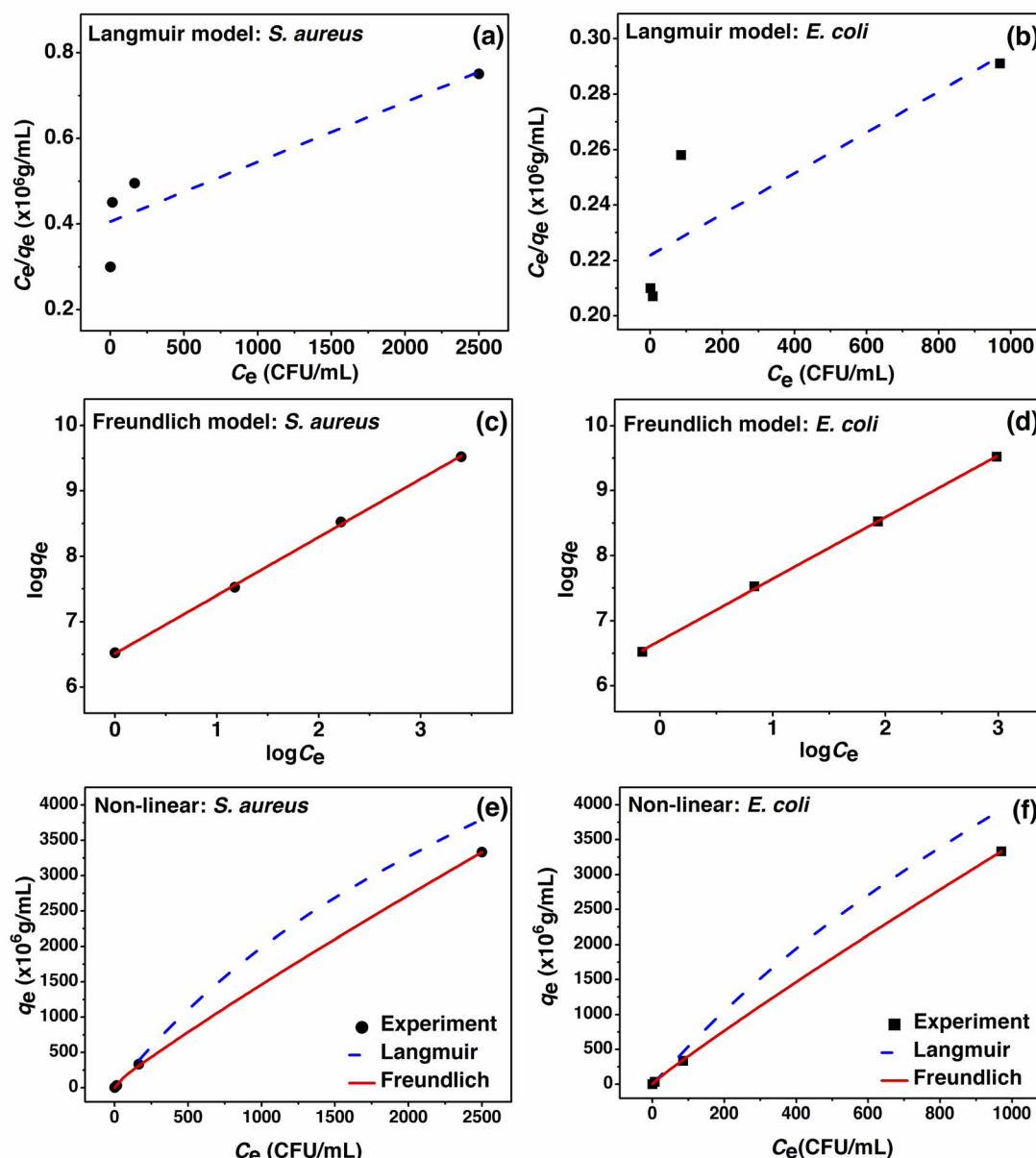
Fig. 9 (a–d) Linear and (e, f) non-linear adsorption isotherm models of PBB on *S. aureus* and *E. coli*.

linear and non-linear models were 0.8344 and 0.9714 for *S. aureus* and 0.7407 and 0.9516 for *E. coli*, respectively. In the Freundlich model, $1/n$ is the constant depicting the adsorption intensity, and $1/n < 1$ means favorable adsorption with different concentrations, where the adsorption capacity will decrease with increasing concentration.[73] For the Freundlich linear model, the $1/n$ values of PBB on *S. aureus* and *E. coli* were 0.8895 and 0.9502, respectively, and the $1/n$ value of *E. coli* was higher than that of *S. aureus*, which meant that PBB had an inhibition capacity on *E. coli* better than that on *S. aureus*. Moreover, the Freundlich linear adsorption constants (K_F) of PBB on *S. aureus* and *E. coli* were 3.2546×10^6 and 4.9136×10^6 (CFU g^{-1}) (L CFU^{-1})$^{1/n}$, respectively. For the Freundlich non-linear model, the $1/n$ values of PBB on *S. aureus* and *E. coli* were 0.8718 and

0.9318, respectively, and the $1/n$ value of *E. coli* was also higher than *S. aureus*, which meant that PBB had a better inhibition capacity on *E. coli* than *S. aureus*. Moreover, the Freundlich non-linear adsorption constants (K_F) of PBB on *S. aureus* and *E. coli* were 3.6357×10^6 and 5.4890×10^6 (CFU g^{-1}) (L CFU^{-1})$^{1/n}$, respectively. The R^2 of Freundlich linear and non-linear models were 0.9994 and 1 for *S. aureus* and 0.9997 and 1 for *E. coli*, respectively. Generally, the R^2 value was used to decide which adsorption isotherm model well explains the adsorption pattern of the adsorbent; thus, a higher R^2 close to 1 was suitably chosen. As a result, the adsorption isotherms of PBB on *S. aureus* and *E. coli* corresponded to Freundlich model in both the linear model (R^2 of 0.9994 and 0.9997) and non-linear models at R^2 equal to 1, which is related to the physiochemical adsorption

Table 6 Equilibrium isotherm parameters of PBB on *S. aureus* and *E. coli*

Isotherm model	Linear		Non-linear	
	S. aureus	*E. coli*	*S. aureus*	*E. coli*
Langmuir model				
q_m (CFU g^{-1})	1×10^{10}	1.4286×10^{10}	1.0083×10^{10}	1.4404×10^{10}
K_L (L CFU^{-1})	0.0003	0.0004	0.0002	0.0003
R^2	0.8344	0.7407	0.9714	0.9516
Freundlich model				
K_F (CFU g^{-1}) (L CFU^{-1})$^{1/n}$	3.2546×10^6	4.9136×10^6	3.6357×10^6	5.4890×10^6
$1/n$	0.8895	0.9502	0.8718	0.9318
R^2	0.9994	0.9997	1	1

process similarly found in a previous study.[39] On comparing the linear and non-linear adsorption isotherm models, their results were found to have close adsorption parameters, which represented the agreement results of linear and non-linear models similarly to other studies.[74–77] As a result, the plotting of the linear and non-linear adsorption isotherm models is necessary to avoid data mistranslation.[78,79]

Adsorption kinetics

The adsorption mechanism including the rate of adsorption to time by the adsorbent can be explained by adsorption kinetics.[80] For the linear model, a pseudo-first order and a pseudo-second order kinetic models were used for the adsorption kinetic studies of PBB by the plotting of $\ln(q_e - q_t)$ *versus* time (t) for the pseudo-first order linear kinetic model and t/q_t *versus* time (t) for the pseudo-second order linear kinetic model, respectively. For the non-linear model, both kinetic models for the plotting of q_t *versus* time (t) are shown in Fig. 10. The adsorption kinetic equilibrium of PBB on *S. aureus* and *E. coli* is represented in Fig. 11, and the adsorption kinetic parameters are reported in Table 7.

For the linear pseudo-first order kinetic model, the adsorption capacities (q_e) of PBB on *S. aureus* and *E. coli* were 8.586×10^6 and 168.662×10^6 CFU g^{-1}, and the k_1 values were 0.055 and 0.033 min^{-1}, respectively. For the linear pseudo-second order kinetic model, the adsorption capacities (q_e) of PBB on *S. aureus* and *E. coli* had the same value of 333.333×10^6 CFU g^{-1}, and the k_2 values were 0.009×10^6 and 0.045×10^6 g CFU^{-1} min^{-1}, respectively. For the non-linear pseudo-first order kinetic model, the adsorption capacities (q_e) of PBB on *S. aureus* and *E. coli* were 9.264×10^6 and 181.989×10^6 CFU g^{-1}, and the k_1 values were 0.078 and 0.046 min^{-1}, respectively. For the non-linear pseudo-second order kinetic model, the adsorption capacities (q_e) of PBB on *S. aureus* and *E. coli* had the same value of 332.138×10^6 CFU g^{-1}, and the k_2 values were 0.010×10^6 and 0.050×10^6 g CFU^{-1} min^{-1}, respectively. Considering the R^2 values of both linear and non-linear kinetic models, the results for both bacterial types corresponded to the pseudo-second order kinetic model with R^2 equal to 1, which meant that the adsorption kinetics of PBB involved chemisorption and was related to the physiochemical interaction of PBB on bacteria similarly reported in a previous study.[39] When

a pseudo-second order kinetic model was chosen as the best fit model to the actual experiment data, the rate constant (k_2) should be mentioned. In Table 6, the rate constant (k_2) of PBB on *S. aureus* was less than *E. coli* in both linear and non-linear kinetics models, which meant that the period of adsorption time on *S. aureus* by PBB was shorter time than that on *E. coli*. The adsorption capacities of bacterial uptake of PBB on *S. aureus* and *E. coli* were gradually increased from 0 to 45 min, and then stable adsorption equilibrium was obtained, as shown in Fig. 11.

Since the plotting of non-linear kinetic models helped to confirm the result of linear plotting to protect the processing data,[81] many previous studies have reported both linear and non-linear kinetic models to confirm their results.[76,77,82,83] Similarly, this study reported and compared the results of linear and non-linear of both the kinetic models, and their results agreed closely with the kinetic parameter values.

Desorption experiments

For industrial applications, the main reason for selecting a new wastewater treatment technology is a reasonable cost with high efficiency; thus, a reusable material of adsorption technique for wastewater treatment is an essential point for long-time reuse. Therefore, the desorption experiments were investigated through several adsorption–desorption cycles to confirm material reusability.

0.01 M HNO$_3$ solution was used for bacterial desorption on PBB, and three cycles of adsorption–desorption were carried out to confirm material reusability. The results confirmed that PBB had high bacterial adsorption and desorption on both bacterial types in all the cycles, as shown in Table 8. For the adsorption process, the adsorption cycles presented high antibacterial efficiencies by PBB in the range of 90 ± 0.3 to $100 \pm 0.0\%$ on *S. aureus* and 93 ± 0.4 to $100 \pm 0.0\%$ on *E. coli*, respectively. For the desorption process, both the bacterial types in adsorbed PBB were almost desorbed by 0.01 M HNO$_3$ solution in the range of 88 ± 0.2 to $100 \pm 0.0\%$ on *S. aureus* and 90 ± 0.4 to $100 \pm 0.0\%$ on *E. coli*, respectively. As a result, the antibacterial efficiencies on *S. aureus* and *E. coli* decreased by 10% and 7%, respectively, whereas the bacteria desorption efficiencies on *S. aureus* and *E. coli* decreased by 12% and 10%, respectively. Therefore, PBB is a potential material with reusability after
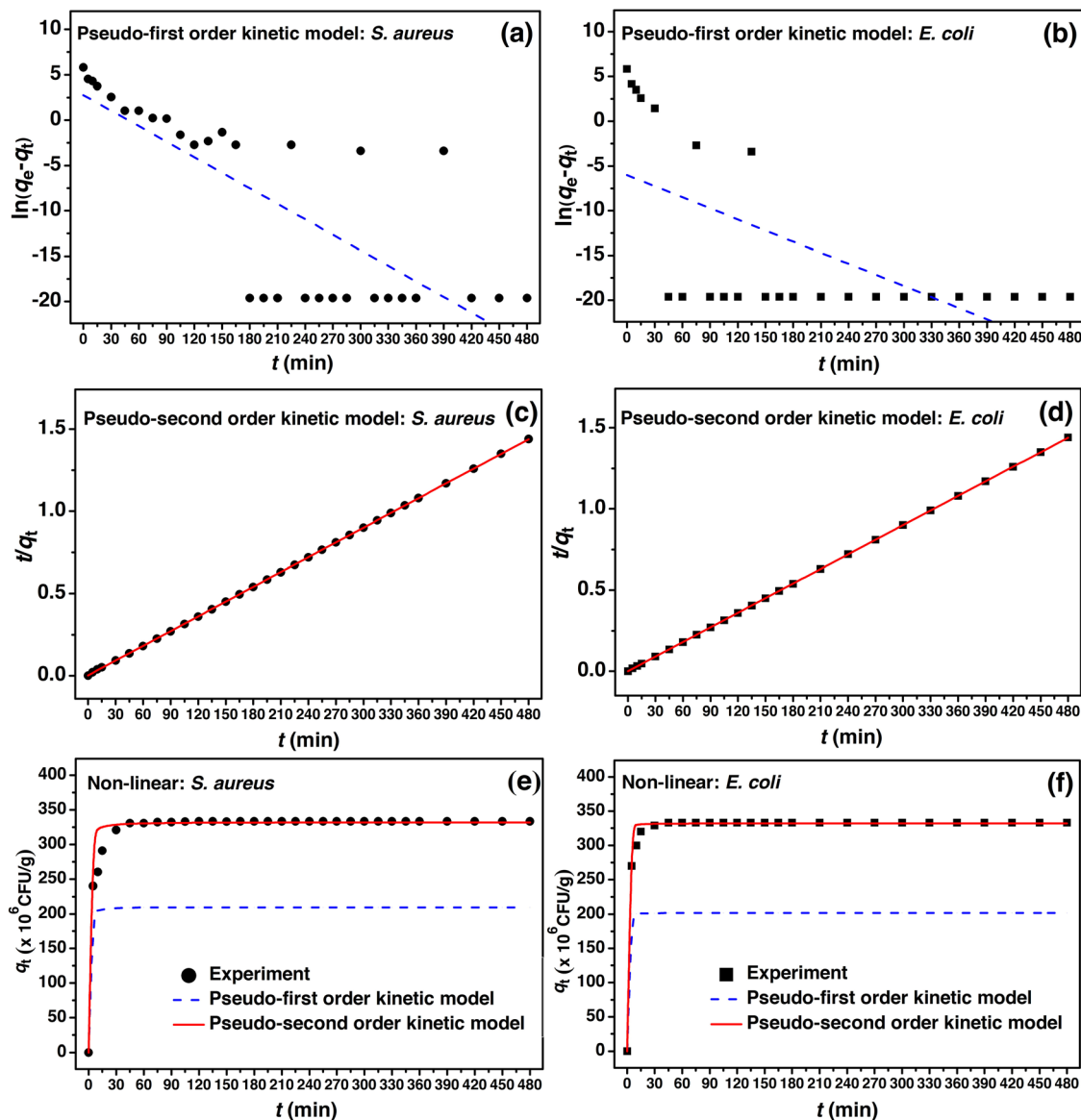
Fig. 10 (a–d) Linear and (e, f) non-linear adsorption kinetic models of PBB on *S. aureus* and *E. coli*.

three continuous adsorption–desorption cycles, and PBB is a suitable material to possibly apply for the disinfection process in wastewater treatment systems in the future.

Possibility of application in industrial wastewater treatment systems

PBB might be used as an antibacterial material for inhibiting *S. aureus* and *E. coli* for applying it as an adsorbent material in the filter tank for contaminated water passed through it for treatment. PBB is not in the treated water for releasing to receiving water, so they might not affect the ecosystem. In particular, the extracted *P. betle* was studied and applied in many applications of food preservations, skincare products, hair, dental, cosmetics, and biopesticides; thus, its use is not dangerous to the ecosystem and environment.

In this study, approximately 3 g *P. betle* leaves were used for synthesizing PBB at a concentration of 300 mg mL^{-1} for treating 100 mL bacterial concentration of *S. aureus* or *E. coli* at 10^6 CFU mL^{-1} at 100% removal in batch experiments. Thus, 30 g *P. betle* could treat 1000 mL bacterial concentration of *S. aureus* or *E. coli* at 10^6 CFU mL^{-1}. As a result, the bacterial concentration and wastewater volume might be used for a possible consideration of wastewater treatment applications and the amount of *P. betle* that should be used.

Moreover, the desorption results confirmed the reusability of PBB for inhibiting both bacterial types. For *S. aureus*, since the antibacterial efficiency of PBB on *S. aureus* was decreased by 10% in 3 cycles or 300 mL in volume, thus, PBB could be reused for more than 30 cycles or 3000 mL in volume for a bacterial concentration of 10^6 CFU mL^{-1}. For *E. coli*, since the antibacterial efficiency of PBB on *E. coli* was decreased by 7% in 3 cycles
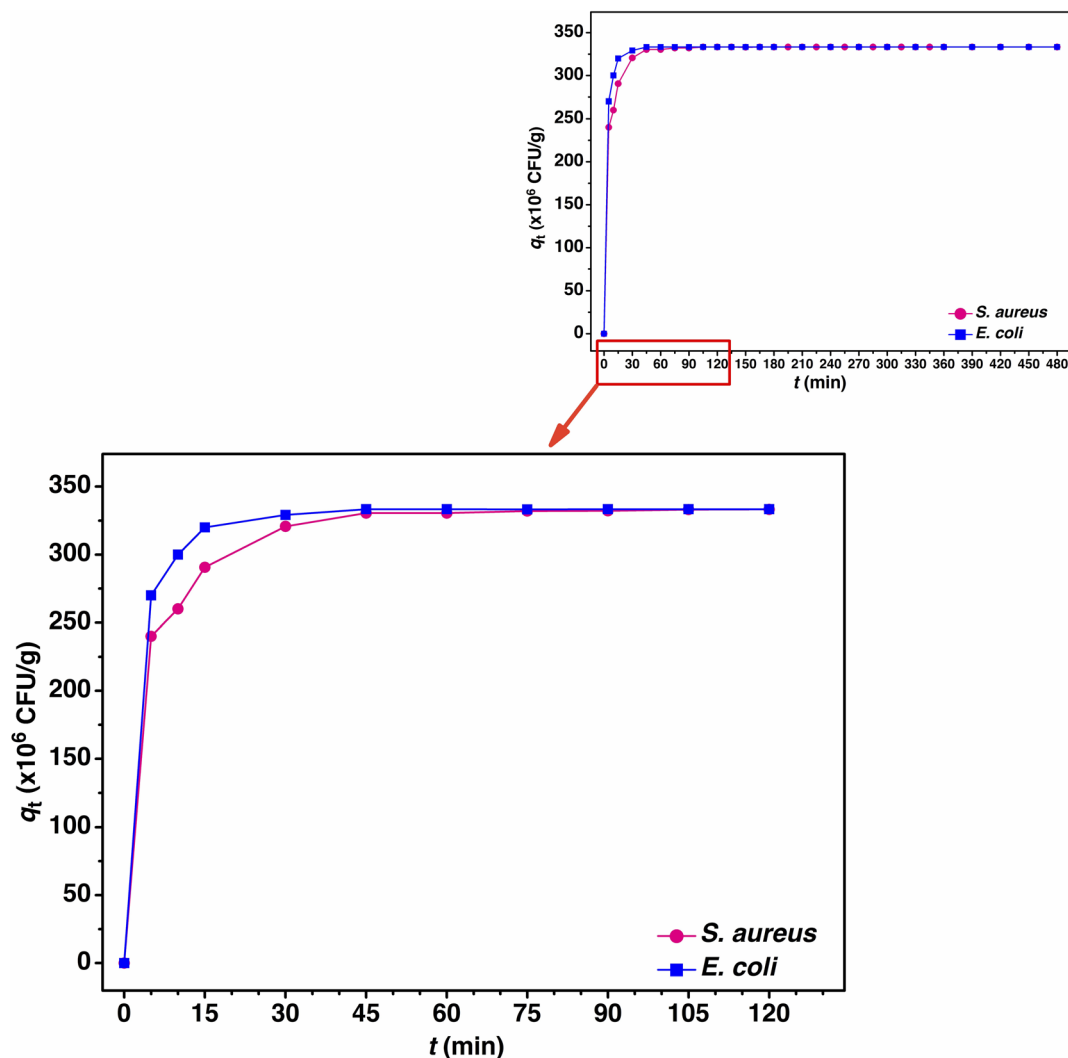
Fig. 11 The adsorption equilibrium of PBB on *S. aureus* and *E. coli*.

or 300 mL in volume; thus, PBB could be reused for more than 42 cycles or 4200 mL in volume for a bacterial concentration of 10^6 CFU mL^{-1}. If the industry needs to treat wastewater of 1000 L in volume, it requires 1 kg and 700 g of *P. betle* leaves for PBB synthesis for inhibiting *S. aureus* and *E. coli*, respectively. Therefore, not only could PBB be used against *S. aureus* and *E.*

coli in wastewater but also it did not leave a big load of waste in the environment.

In addition, although *P. betle* is mostly grown in many countries in Southeast Asia such as Thailand, Malaysia, Vietnam, India, and Sri Lanka, it can also grow everywhere in the world with appropriate conditions of tropical wet climate and slightly acidic, sandy-loamy, or lightly damp soils. Thus, *P. betle* leaves have enough raw materials for PBB synthesis for use as

Table 7 Adsorption kinetic parameters of PBB on *S. aureus* and *E. coli*

Kinetic model	Linear		Non-linear	
	S. aureus	*E. coli*	*S. aureus*	*E. coli*
Pseudo-first order kinetic model				
k_1 (min^{-1})	0.055	0.033	0.078	0.046
q_e ($\times 10^6$ CFU g^{-1})	8.586	168.662	9.264	181.989
R^2	0.571	0.316	0.588	0.330
Pseudo-second order kinetic model				
k_2 ($\times 10^6$ g CFU^{-1} min^{-1})	0.009	0.045	0.010	0.050
q_e ($\times 10^6$ CFU g^{-1})	333.333	333.333	332.138	332.138
R^2	1	1	1	1

Table 8 The adsorption and desorption of PBB on *S. aureus* and *E. coli* in three cycles

Bacterial	Cycle	Adsorption (%)	Desorption (%)
S. aureus	1	100 ± 0.0	100 ± 0.0
	2	96 ± 0.4	93 ± 0.4
	3	90 ± 0.3	88 ± 0.2
E. coli	1	100 ± 0.0	100 ± 0.0
	2	98 ± 0.3	95 ± 0.3
	3	93 ± 0.4	90 ± 0.4

antibacterial adsorbents in world. Furthermore, the synthesis method of PBB is not complicated and can be applied for industrial manufacturing as an alternative product of antibacterial materials for killing contaminated bacteria, especially *S. aureus and E. coli* in wastewater.

Conclusion

This study extracted *P. betle* powder (PBP) and synthesized *P. betle* beads (PBB) for antibacterial activity against *S. aureus* and *E. coli*. The FESEM-FIB images show that PBP had a porous and rough surface, whereas PBB had a spherical shape with coarse surfaces. EDX analysis illustrated that the four main chemical compositions of PBP and PBB were carbon (C), oxygen (O), calcium (Ca), and chlorine (Cl), and O–H, C–H, N–H, and C–O were the four main functional groups of PBP and PBB were identified by FTIR. The extraction yield of *P. betle* was 11.30%, and total phenolic, flavonoid, and tannin contents of *P. betle* were 201.55 ± 0.31 mg GAE per g, 56.86 ± 0.14 mg RE per g, and 41.76 ± 1.32 mg CE per g, respectively. The six main compounds of eugenol, quercetin, apigenin, kaempferol, ascorbic acid, and hydroxychavicol and nine trace compounds of rutin, syringic acid, catechin, sinapic acid, *p*-coumaric acid, caffeic acid, ferrulic acid, myrecetin, and gallic acid were detected by HPLC analysis. The results of disc diffusion assay by EPB and PBB confirmed that the extracted *P. betle* potentially inhibited *S. aureus* and *E. coli*. For antibacterial batch experiments, the optimum condition of PBB for 100% bacterial removal on both bacterial types was 0.3 g, 6 h, pH 7, and 10^6 CFU mL^{-1}. The adsorption isotherms and kinetics of PBB on *S. aureus* and *E. coli* corresponded to the Freundlich model, and the pseudo-second order kinetic model was related to chemisorption and physiochemical interaction of PBB on both bacterial types. Moreover, the desorption experiments confirmed the material reusability. Finally, PBB was a potential material for inhibiting *S. aureus* and *E. coli*, and could possibly be applied in the disinfection process of wastewater treatment systems in the future.

For future works, other bacterial types of Gram-positive and Gram-negative bacteria should be investigated by PBB as competing bacterial contaminations in real wastewater, and other contaminated compounds of organic matters or nutrients cannot be ignored. Moreover, continuous flow study is recommended to explore whether PBB can be possibly applied for the disinfection process of a real wastewater system.

Data availability

The raw/processed data required to reproduce these findings cannot be shared at this time due to legal or ethical reasons.

The raw/processed data required to reproduce these findings cannot be shared at this time as the data also forms part of an ongoing study.

Author contributions

Pimploy Ngamsurach: investigation, visualization, writing – original draft Pornsawai Praipipat: supervision, conceptualization, funding acquisition, validation, investigation, methodology, visualization, writing – original draft, writing – review & editing.

Conflicts of interest

The authors declare that they have no known competing financial interests or personal relationships that could have appeared to influence the work reported in this paper.

Acknowledgements

References

1 L. Schweitzer and J. Noblet, *Green Chem.*, 2018, 261–290.

2 A. E. Evans, J. Mateo-Sagasta, M. Qadir, E. Boelee and A. Ippolito, *Curr. Opin. Environ. Sustain.*, 2019, **36**, 20–27.

3 A. Kozajda, K. Jezak and A. Kapsa, *Environ. Sci. Pollut. Res.*, 2019, **26**, 34741–34753.

4 M. Schaechter, S. Diego and S. Diego, *Escherichia coli, Encyclopedia of Microbiology*, 3rd edn, 2009, pp. 125–132.

5 J. Wang, J. Shen, D. Ye, X. Yan, Y. Zhang, W. Yang, X. Li, J. Wang, L. Zhang and L. Pan, *Environ. Pollut.*, 2020, **262**, 114665.

6 S. Basak and P. Guha, *LWT–Food Sci. Technol.*, 2017, **80**, 510–516.

7 A. Roy and P. Guha, *J. Food Process. Preserv.*, 2018, **42**, 1–7.

8 F. Rodrigues, A. Palmeira-de-Oliveira, J. das Neves, B. Sarmento, M. H. Amaral and M. B. Oliveira, *Ind. Crops Prod.*, 2013, **49**, 634–644.

9 N. Joshi, K. Patidar, R. Solanki and V. Mahawar, *Int. J. Green Pharm.*, 2018, **12**, S835–S839.

10 M. A. Lugo-Flores, K. P. Quintero-Cabello, P. Palafox-Rivera, B. A. Silva-Espinoza, M. R. Cruz-Valenzuela, L. A. Ortega-Ramirez, G. A. Gonzalez-Aguilar and J. F. Ayala-Zavala, *Biomedicines*, 2021, **9**(11), 1669.

11 P. Yushananta and M. Ahyanti, *Open Access Maced. J. Med. Sci.*, 2021, **9**, 895–900.

12 P. Niyomkam, S. Kaewbumrung, S. Kaewnpparat and P. Panichayupakaranant, *Pharm. Biol.*, 2010, **48**, 375–380.

13 S. Nanasombat and N. Teckchuen, *J. Med. Plants Res.*, 2009, **3**, 443–449.

14 K. Subramani, B. K. Shanmugam, S. Rangaraj, V. Murugan, S. Srinivasan, O. K. Awitor, C. Massard and R. Venkatachalam, *J. Coat. Technol. Res.*, 2020, **17**, 1363–1375.

15 A. Ali, X. Y. Lim and P. F. Wahida, *J. Herb. Med.*, 2018, **14**, 29–34.

16 D. L. Valle, J. I. Andrade, J. J. M. Puzon, E. C. Cabrera and W. L. Rivera, *Asian Pac. J. Trop. Biomed.*, 2015, **5**, 532–540.

17 V. Dwivedi and S. Tripathi, *J. Pharmacogn. Phytochem.*, 2014, **3**, 93–98.

18 Y. Lin, K. Xiong, Z. Lu, S. Liu, Z. Zhang, Y. Lu, R. Fu and D. Wu, *Chem. Commun.*, 2017, **53**, 9777–9780.

19 W. P. T. D. Perera, R. K. Dissanayake, U. I. Ranatunga, N. M. Hettiarachchi, K. D. C. Perera, J. M. Unagolla, R. T. De Silva and L. R. Pahalagedara, *RSC Adv.*, 2020, **10**, 30785–30795.

20 S. Moniri Javadhesari, S. Alipour, S. Mohammadnejad and M. R. Akbarpour, *Mater. Sci. Eng. C*, 2019, **105**, 110011.

21 R. B. Asamoah, A. Yaya, B. Mensah, P. Nbalayim, V. Apalangya, Y. D. Bensah, L. N. W. Damoah, B. Agyei-Tuffour, D. Dodoo-Arhin and E. Annan, *Results Mater.*, 2020, **7**, 100099.

22 M. Thukkaram, S. Sitaram, S. K. Kannaiyan and G. Subbiahdoss, *Int. J. Biomater.*, 2014, 716080.

23 X. Xue, Y. Wang and H. Yang, *Appl. Surf. Sci.*, 2013, **264**, 94–99.

24 L. M. Anaya-Esparza, E. Montalvo-González, N. González-Silva, M. D. Méndez-Robles, R. Romero-Toledo, E. M. Yahia and A. Pérez-Larios, *Materials*, 2019, **12**(5), 698.

25 M. Ikram, E. Umar, A. Raza, A. Haider, S. Naz, A. Ul-Hamid, J. Haider, I. Shahzadi, J. Hassan and S. Ali, *RSC Adv.*, 2020, **10**, 24215–24233.

26 D. Paul, S. Mangla and S. Neogi, *Mater. Lett.*, 2020, **271**, 127740.

27 P. P. Mahamuni, P. M. Patil, M. J. Dhanavade, M. V. Badiger, P. G. Shadija, A. C. Lokhande and R. A. Bohara, *Biochem. Biophys. Rep.*, 2019, **17**, 71–80.

28 M. I. Jahanger, N. A. Shad, M. M. Sajid, K. Akhtar, Y. Javed, A. Ullah, M. A. Hassan, M. H. Sarwar, M. Sarwar and M. Sillanpää, *React. Kinet., Mech. Catal.*, 2022, **135**, 499–510.

29 M. I. Nabila and K. Kannabiran, *Biocatal. Agric. Biotechnol.*, 2018, **15**, 56–62.

30 R. Li, Z. Chen, N. Ren, Y. Wang, Y. Wang and F. Yu, *J. Photochem. Photobiol., B*, 2019, **199**, 111593.

31 A. Jain, F. Ahmad, D. Gola, A. Malik, N. Chauhan, P. Dey and P. K. Tyagi, *Environ. Nanotechnol., Monit. Manage.*, 2020, **14**, 100337.

32 S. Vasantharaj, S. Sathiyavimal, M. Saravanan, P. Senthilkumar, K. Gnanasekaran, M. Shanmugavel, E. Manikandan and A. Pugazhendhi, *J. Photochem. Photobiol., B*, 2019, **191**, 143–149.

33 A. K. M. Atique Ullah, A. N. Tamanna, A. Hossain, M. Akter, M. F. Kabir, A. R. M. Tareq, A. K. M. Fazle Kibria, M. Kurasaki, M. M. Rahman and M. N. I. Khan, *RSC Adv.*, 2019, **9**, 13254–13262.

34 R. Ishwarya, B. Vaseeharan, S. Kalyani, B. Banumathi, M. Govindarajan, N. S. Alharbi, S. Kadaikunnan, M. N. Al-anbr, J. M. Khaled and G. Benelli, *J. Photochem. Photobiol., B*, 2018, **178**, 249–258.

35 A. Ananda, T. Ramakrishnappa, S. Archana, L. S. Reddy Yadav, B. M. Shilpa, G. Nagaraju and B. K. Jayanna, *Mater. Today: Proc.*, 2021, **49**, 801–810.

36 S. Ramli, S. Radu, K. Shaari and Y. Rukayadi, *BioMed Res. Int.*, 2017, 9024246.

37 W. Yuan and H. G. Yuk, *Food Microbiol*, 2018, **72**, 176–184.

38 D. Nigussie, G. Davey, B. A. Legesse, A. Fekadu and E. Makonnen, *BMC Complementary Med. Ther.*, 2021, **21**, 1–10.

39 P. Ngamsurach and P. Praipipat, *ACS Omega*, 2021, **6**, 32215–32230.

40 V. L. Singleton, R. Orthofer and R. M. Lamuela-Raventós, *Methods Enzymol.*, 1999, **299**, 152–178.

41 J. Zhishen, T. Mengcheng and W. Jianming, *Food Chem.*, 1999, **64**, 555–559.

42 B. Sun, J. M. Ricardo-da-Silva and I. Spranger, *J. Agric. Food Chem.*, 1998, **46**, 4267–4274.

43 I. Langmuir, *J. Am. Chem. Soc.*, 1918, **40**, 1361–1403.

44 H. Freundlich, *J. Phys. Chem.*, 1906, **57**, 385–470.

45 S. Lagergren, *K. Sven. Vetenskapsakad. Handl.*, 1898, **24**, 1–39.

46 Y. S. Ho and G. Mckay, *Process Biochem.*, 1999, **34**, 451–465.

47 V. P. B. Rekha, M. Kollipara, S. Gupta, Y. Bharath and K. K. Pulicherla, *Am. J. Ethnomed.*, 2015, **1**, 276–289.

48 T. Varadavenkatesan, R. Selvaraj and R. Vinayagam, *J. Mol. Liq.*, 2016, **221**, 1063–1070.

49 T. P. Singh, G. Chauhan, R. K. Agrawal and S. K. Mendiratta, *J. Food Meas. Charact.*, 2019, **13**, 466–475.

50 L. Muruganandam, A. Krishna, J. Reddy and G. S. Nirmala, *Resour. Technol.*, 2017, **3**, 385–393.

51 N. H. Nguyen, T. T. Y. Nhi, N. T. Van Nhi, T. T. T. Cuc, P. M. Tuan and D. H. Nguyen, *J. Nanomater.*, 2021, **2021**, 5518389.

52 U. Gaware, V. Kamble and B. Ankamwar, *Int. J. Electrochem.*, 2012, **2012**, 1–6.

53 M. M. O. Rashid, M. S. Islam, M. A. Haque, M. A. Rahman, M. T. Hossain and M. A. Hamid, *Iran. J. Pharm. Res.*, 2016, **15**, 591–597.

54 N. T. Thuong, H. T. Ngoc Bich, C. N. H. Thuc, B. T. P. Quynh and L. Van Minh, *ChemistrySelect*, 2019, **4**, 8150–8157.

55 L. Nouri, A. Mohammadi Nafchi and A. A. Karim, *Ind. Crops Prod.*, 2014, **62**, 47–52.

56 L. T. T. Nguyen, T. T. Nguyen, H. N. Nguyen and Q. T. P. Bui, *Eng. Reports*, 2020, **2**, 2–9.

57 H. V. Annegowda, P. Y. Tan, M. N. Mordi, S. Ramanathan, M. R. Hamdan, M. H. Sulaiman and S. M. Mansor, *Food Anal. Methods*, 2013, **6**, 715–726.

58 U. Taukoorah, N. Lall and F. Mahomoodally, *S. Afr. J. Bot.*, 2016, **105**, 133–140.

59 A. Noor, M. Al Murad, A. Jaya Chitra, S. N. Babu and S. Govindarajan, *Food Biosci.*, 2022, **47**, 101715.

60 J. A. Khan and N. Kumar, *J. Pharm. Biomed. Sci.*, 2011, **11**, 1–3.

61 B. Jayalakshmi, K. A. Raveesha, M. Murali and K. N. Amruthesh, *Int. J. Pharm. Pharm. Sci.*, 2015, **7**(10), 23–29.

62 P. Kulnanan, J. Chuprom, T. Thomrongsuwannakij, C. Romyasamit, S. Sangkanu, N. Manin, V. Nissapatorn, M. de Lourdes Pereira, P. Wilairatana, W. Kitpipit and W. Mitsuwan, *Arch. Microbiol.*, 2022, **204**, 1–14.

63 K. N. Akter, P. Karmakar, A. Das, S. N. Anonna, S. A. Shoma and M. M. Sattar, *Avicenna J. Phytomed.*, 2014, **4**, 320–329.

64 D. L. Valle, E. C. Cabrera, J. J. M. Puzon and W. L. Rivera, *PLoS One*, 2016, **11**, 1–14.

65 A. A. Ali Almahdi and Y. Kumar, *Int. J. Curr. Microbiol. Appl. Sci.*, 2019, **8**, 2009–2019.

66 B. Kaveti, L. Tan, T. S. Kuan and M. Baig, *J. Pharm. Teach.*, 2011, **2**, 129–132.

67 R. R. Lubis, M. Hawley and D. D. Wahyuni, *Am. J. Clin. Exp. Immunol.*, 2020, **9**, 1–5.

68 F. U. Ermawati, R. Sari, N. P. Putri, L. Rohmawati, D. H. Kusumawati, Munasir and Z. A. I. Supardi, *J. Phys.: Conf. Ser.*, 2021, **1951**, 012004.

69 A. Budiman and D. L. Aulifa, *Pharmacogn. J.*, 2020, **12**, 473–477.

70 A. Datta, S. Ghoshdastidar and M. Singh, *Int. J. Pharma Sci. Res.*, 2011, **2**, 104–109.

71 W. K. Jung, H. C. Koo, K. W. Kim, S. Shin, S. H. Kim and Y. H. Park, *Appl. Environ. Microbiol.*, 2008, **74**, 2171–2178.

72 Y. L. Ying, S. Y. Pung, M. T. Ong and Y. F. Pung, *J. Ind. Eng. Chem.*, 2018, **67**, 437–447.

73 M. Rezakazemi and Z. Zhang, *Desulfurization Materials*, 2018, vol. 2.

74 P. Ganguly, R. Sarkhel and P. Das, *Surf. Interfaces*, 2020, **20**, 100616.

75 Q. Sun and B. Chen, *Ind. Eng. Chem. Res.*, 2020, **59**, 16838–16850.

76 A. Threepanich and P. Praipipat, *J. Environ. Chem. Eng.*, 2021, **9**, 106007.

77 A. Threepanich and P. Praipipat, *Environ. Sci. Pollut. Res.*, 2022, **29**, 46077–46090.

78 A. D. Zand and M. R. Abyaneh, *Sustain. Environ. Res.*, 2020, **30**, 1–16.

79 R. Yang, J. Aoqi, S. He, Q. Hu, M. Sun, T. Dong, Y. Hou and S. Zhou, *Chem. Eng. J.*, 2020, **406**, 125982.

80 A. M. Aljeboree, A. N. Alshirifi and A. F. Alkaim, *Arab. J. Chem.*, 2017, **10**, S3381–S3393.

81 P. Paluri, K. A. Ahmad and K. S. Durbha, *Biomass Convers. Biorefin.*, 2022, **12**, 4031–4048.

82 F. Cao and J. Shen, *J. Chem. Eng. Data*, 2019, **64**, 5622–5629.

83 D. M. Salh, B. K. Aziz and S. Kaufhold, *Silicon*, 2020, **12**, 87–99.